Observed Impacts of Aerosol Regimes on Energy and Carbon Fluxes in the Amazon Forest

Mariano A.B. da Rocha[1], Cléo Q. Dias-Júnior[1, 2, 3], Anne C.S. Mendonça[3], Julia C.P. Cohen[1], Flávio A.F. D'Oliveira[2], Christopher Pöhlker[4], Subha Raj[4], Alessandro C. de Araujo[1, 5], Marco A. Franco[6], Paulo Artaxo[7], Carlos A. Quesada[8], and Rafael S. Palácios[9]

[1]Graduate Program in Environmental Sciences, Federal University of Pará, Belém, Pará, Brazil
[2]Department of Physics, Federal Institute of Pará, Belém, Pará, Brazil
[3]Graduate Program in Climate and Environment, National Institute of Amazonian Research, Manaus, Amazonas, Brazil
[4]Multiphase Chemistry Department, Max Planck Institute for Chemistry, Mainz, Germany
[5]Empresa Brasileira de Pesquisa Agropecuária, Belém, Brazil
[6]Department of Atmospheric Sciences, Institute of Astronomy, Geophysics and Atmospheric Sciences, University of São Paulo, São Paulo, Brazil
[7]Institute of Physics, University of São Paulo, São Paulo, Brazil
[8]National Institute of Amazonian Research, Manaus, Amazonas, Brazil
[9]Institute of Geosciences and Faculty of Meteorology, Federal University of Pará, Belém, Pará, Brazil

Correspondence: Cléo Q. Dias-Júnior (cleo.quaresma@ifpa.edu.br)

Abstract. Atmospheric aerosols play a crucial role in modulating the energy available to the Earth's surface, influencing the hydrological cycle, ecosystems, and climate. In the Amazon, previous studies have mainly examined how aerosols scatter and absorb radiation. ~~, enhancing diffuse radiation and influencing gross primary productivity.~~ However, little is known about their interactions with energy partitioning (i.e., sensible and latent heat fluxes). Here, we investigate how regimes of high ($AOD > 0.40$) and low ($AOD < 0.13$) aerosol optical depth (AOD) affect surface energy and carbon dioxide (CO_2) fluxes in an undisturbed Amazon rainforest. For this, we used long-term meteorological measurements from the Amazon Tall Tower Observatory (ATTO) collected between 2016 and 2022. We find that enhanced aerosol presence reduces both sensible heat flux and energy available for evapotranspiration by approximately ~~10%~~ 13.5% and 2.1% respectively, while ~~decreasing~~ increasing CO_2 uptake~~fluxes~~ (i.e., CO_2 flux becoming more negative) by about 39.5%. ~~which suggests enhanced carbon assimilation by the forest.~~ The impact of aerosols on turbulent surface fluxes is reflected in a cooling of approximately ~~0.5~~ 0.9 °C at the canopy top, caused by a ~~5.6~~ 2.8% reduction in incoming shortwave radiation. These results demonstrate that aerosols modify turbulent energy exchange, with consequences for the forest microclimate and the coupled carbon and water cycles. ~~It highlights the critical role of aerosols in the functioning of the ecosystem.~~

1 Introduction

Atmospheric aerosols, which are defined as solid or liquid particles suspended in the air (Seinfeld and Pandis, 2006), play a multifaceted role in the Earth system. They influence the atmospheric cycle (Lohmann and Feichter, 2005; Rap et al., 2013;

Gavrouzou et al., 2023), the hydrological cycle (Miller et al., 2004; Lau et al., 2005; Suzuki et al., 2017), and ecosystem processes (Kanakidou et al., 2018; Artaxo et al., 2022; Karthick Raja Namasivayam et al., 2024).

In the atmosphere, aerosols interact directly with solar radiation through scattering and absorption processes. These interactions influence the Earth's energy balance and, consequently, the climate (Liu et al., 2020). Aerosols also act indirectly by interacting with clouds, acting as cloud condensation nuclei. This interaction alters the albedo, formation, microphysics, and lifetime of clouds, thereby impacting global climate patterns (Andreae et al., 2004; Eltbaakh et al., 2012; Wang and Yi, 2024).

In the hydrological cycle, aerosols reduce the intensity of precipitation through complex, partially nonlinear processes that involve suppression of convection through mechanisms of aerosol-radiation interaction that stabilize the atmosphere, particularly at levels of aerosol optical depth (AOD) greater than 0.40 (Herbert and Stier, 2023). This results in a greater number of cloud droplets with a radius of less than 14 μm forming, which are insufficient for precipitation (Ramanathan et al., 2001; Gonçalves et al., 2015). In addition, they influence downdrafts, ~~altering~~ which alter the concentration of gases near the surface (D'Oliveira et al., 2022). Aerosols also reduce global evapotranspiration, which has a more significant impact on tropical forests (Palácios et al., 2024).

In forest ecosystems, high concentrations of aerosols can increase the intensity of diffuse radiation, which positively impacts photosynthetic rates (Li et al., 2025). This phenomenon, known as diffuse fertilization, mainly benefits shaded areas, allowing them to carry out photosynthesis more efficiently (Kanniah et al., 2012).

The Amazon region, home to the world's largest tropical rainforest, has been the site of significant research on the intricate relationship between aerosols, the biosphere, the atmosphere, and human activities. Since the 1980s, several scientific projects have been conducted in the region to better understand these interactions (Orsini et al., 1896; Artaxo and Orsini, 1987; Harriss et al., 1988; Avissar et al., 2002). Other studies have deepened our knowledge of the formation, transformation and impact of aerosols, particularly on clouds and precipitation (Yokelson et al., 2007; Martin et al., 2010; Brito et al., 2014; Machado et al., 2014; Martin et al., 2017; Machado et al., 2021; Franco et al., 2022). The Amazon Tall Tower Observatory (ATTO) project has recently played an instrumental role in monitoring long-term changes and in understanding the role of aerosols in global climate and the Amazon ecosystem (Andreae et al., 2015; Cecchini et al., 2025).

Aerosols in the Amazon are mainly composed of organic carbon, accounting for more than 80% of their mass (Artaxo et al., 2022). This proportion varies seasonally and can exceed 90% during the burning seasons. During the wet season, aerosol concentrations are low and similar to those of concentrations above the ocean (Pöhlker et al., 2018). However, in the dry season, fires drastically increase the aerosol load, which affects cloud formation and precipitation. These particles also alter the radiative balance, significantly affecting carbon absorption by the forest (Rodrigues et al., 2024). Changes in land use and an increase in fires not only lead to higher levels of pollution, but also reduce rainfall efficiency and modify the regional climate. This creates a positive feedback ~~loop~~ that can result in two different climatic states: one humid and sparsely Polluted and the other dry and highly Polluted (Andreae et al., 2004; Pöhlker et al., 2019).

Despite advances in understanding aerosol-biosphere-atmosphere interactions in the Amazon, the impact of these particles on energy and radiation partitioning and CO_2 fluxes is still unclear. Using numerical simulations for the Amazon basin, Braghiere et al. (2020) showed that there are considerable uncertainties about the influence of aerosols on the surface energy

balance. Their simulations also revealed that, in a scenario without aerosols (AOD = 0), the sensible and latent heat fluxes were higher than those measured experimentally, resulting in higher surface temperatures. Furthermore, recent studies, such as those by Blichner et al. (2024), reveal that numerical models still fail to accurately portray the interaction between aerosols and thermal effects in the Amazon. This is mainly due to the models' inability to adequately capture the relationship between temperature and organic aerosol concentrations.

The aim of this study was to evaluate the influence of aerosols on energy and carbon fluxes, ~~(net radiation – R_n, sensible heat – H, and latent heat – LE) and mass flux (carbon dioxide flux – FCO_2)~~ at the forest-atmosphere interface in an undisturbed region of the Amazon. Using in situ measurements, the study analyzed the period between 2016 and 2022, contributing to our understanding of processes involving the interaction between atmospheric aerosols and the energy balance in an area of pristine Amazon forest. To date, we are unaware of any studies that have used a long-term, purely observational approach to examine ~~experimental data measured close to the surface to examine~~ the relationship between aerosols and energy partitioning directly from surface-based measurements in the Amazon.

2 Material and Methods

2.1 Experimental site

The data used in this study were collected as part of the ATTO project, a bilateral initiative between Brazil and Germany. Since 2012, ATTO has carried out continuous measurements, as described by Andreae et al. (2015), located in an area of pristine tropical forests in the central Amazon (Figure 1), which contains ~~several measurement towers, including~~ the Instant Tower of 81 meters (-2.1441° S, -58.9999° W). ~~and the Tall Tower of 325 meters (-2.1459° S, -59.0056° W).~~

The ~~ATTO~~ Instant tower~~s are~~ is located 150 km from the city of Manaus in the state of Amazonas, Brazil, at an altitude of 120 meters above sea level on a plateau covered by terra firme forests with an average crown height of 40 meters (Gomes Alves et al., 2023). In this landscape, wind speeds are relatively low, around 1 ms^{-1} immediately above the forest canopy, and above the canopy, the wind speed increases logarithmically with height (Santana et al., 2016). The main wind direction at the site is from the NE – E. It passes through areas of minimal anthropogenic influence in the northeast, a Clean fetch region covered by tropical forests (Pöhlker et al., 2019).

The climate is tropical humid~~, divided into~~ and characterized by two seasons (wet and dry), driven by ~~with the predominant origins of the air masses due to the large~~ seasonal shifts of the Intertropical Convergence Zone over the Amazon Basin (Andreae et al., 2015). The wet season is characterized by more than 200 mm of rainfall per month and an average temperature of around 25 °C at the forest-atmosphere interface. In contrast, the dry season sees less than 100 mm of rainfall per month and an average temperature of around 27.7 °C (Schmitt et al., 2023).

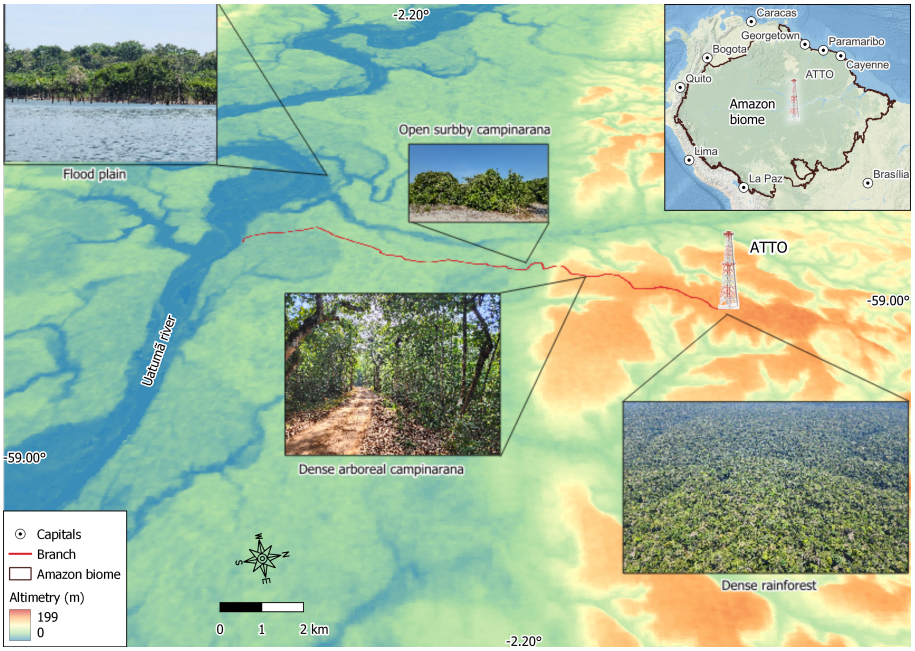

Figure 1. Amazon Tall Tower Observatory (ATTO) in central Amazonia, which has different landscapes along the topographic gradient, including floodplains, shrubby campinarana, dense arboreal campinarana, and dense ombrophilous forests. It is close to the Uatumã River, which runs in an NW-SE direction and is a tributary of the left bank of the Amazon River. Altimetry data by NASA JPL (2020) and vetorial data by RAISG (2023).

2.2 Experimental data

The dataset used in this study was measured at the ATTO site from 2016 to 2022 (see Table 1). Wind speed, sensible heat flux (H), latent heat flux (LE), and carbon dioxide flux (FCO_2) data were calculated as 30-minute averages using EddyPro® software (LI-COR) ~~(LiCor)~~, as derived from fast-response sonic anemometers, according to Fratini and Mauder (2014). The other variables (radiation, thermodynamics and aerosols) were obtained as 30-minute averages, including net radiation (R_n) and its radiative components: incoming and outgoing shortwave radiation (SW_{in} and SW_{out}), and atmospheric and terrestrial longwave radiation (LW_{atm} and LW_{terr}), respectively. Additionally, diffuse shortwave radiation (SW_d) was measured using a SPN1 Pyranometer (Delta-T Devices) installed at 75 m above ground level. However, SW_d data were available only for 2021, prior to this year, SW_d was not measured at the ATTO site, and data from 2022 were excluded due to technical issues with the sensor.

Based on Andreae et al. (2015) and Pöhlker et al. (2016), these data were organized by seasonality into four periods: (i) the wet season (February to May), which has a cleaner atmosphere, (ii) the wet-dry transition (June to July), (iii) the dry season (August to November), which has higher levels of pollution, and (iv) the dry-wet transition (December to January).

Table 1. Variables and the methods used to obtain them.(*) Calculations according to Bolton (1980).

Type of Variable	Variable	Unit	Hight(m)	Method of production	Data sampling rate
Radiation	Short Wave Radiation (SW)	$\mathrm{W\,m^{-2}}$	75	Kipp&Zonen CMP21	1 min
	Long Wave Radiation (LW)	$\mathrm{W\,m^{-2}}$	75	Kipp&Zonen CGR4	1 min
	Net Radiation (R_n)	$\mathrm{W\,m^{-2}}$	75	Kipp & Zonen NR-LITE2	1 min
Thermodynamics	Air temperature (T)	°C	80	GALLTEC-MELA IAK I-Series	1 min
	Infrared surface temperature	°C	35	Campbell Scientific TIR radiometer (IR120)	1 min
	Relative humidity (RH)	%	80	GALLTEC MELA IAK I-Series	1 min
	Air Pressure (Patm)	hPa	80	YOUNG 61302V	1 min
	Wind speed	$\mathrm{m\,s^{-1}}$	80	CSAT3B & THIES 4.3830	1 min
	Vapor pressure deficit (VPD)	hPa	-	Calculation*	1 min
	Mixing ratio (r)	g of vapor/kg of dry air	-	Calculation*	1 min
	Soil temperature (Ts)	°C	0.1	Campbell Thermistor 108	10 min
	Soil moisture (h)	$\mathrm{m^3\,m^{-3}}$	0.1	Campbell CS615	10 min
Flux	Sensible Heat (H)	$\mathrm{W\,m^{-2}}$	80	CSAT3B/LI-7200RS	10 Hz
	Latent Heat (LE)	$\mathrm{W\,m^{-2}}$	80	CSAT3B/LI-7200RS	10 Hz
	Carbon dioxide (FCO_2)	$\mu\mathrm{mol\,m^{-2}\,s^{-1}}$	80	CSAT3B/LI-7200RS	10 Hz
	Ground heat (G)	$\mathrm{W\,m^{-2}}$	0.05	Hukseflux HFP01	10 min
Aerosols	Aerosol Optical Depth 500 nm (AOD)	-	80	CIMEL Sun Photometer CE318-T	Variable rate

~~Initially, the database containing the variables in Table 1 had 10,890 rows, each of which has values averaged over 30 minutes. However, some filters were applied: i)~~ To eliminate cloud interference and investigate the role of aerosols in surface energy fluxes, the central objective of this study, we used data from the Aerosol Robotic Network (AERONET) at the ATTO site, specifically AOD (version 3, level 2). These data are free of cloud contamination due to pre and post-field calibration (Giles et al., 2019). Based on this, 30-minute averages were calculated between 2016 and 2022 for which AOD data from AERONET were available, the initial combined dataset comprised 10,890 observations, including all variables listed in Table 1. This matched dataset served as the starting point for the subsequent quality control and filtering procedures. First, the turbulent fluxes underwent quality control following Foken et al. (2004)~~.~~, who defined that only ~~Only~~ data with flags "0" (best quality) and "1" (acceptable for general analysis) should be used; data with flag "2" (poor quality) were discarded ~~ii) the presence of clouds interferes with radiation balance and energy partitioning. To eliminate cloud interference and investigate the role of aerosols in surface energy fluxes, the central objective of this study, data from the Aerosol Robotic Network (AERONET) at the ATTO site, specifically AOD (version 3, level 2). These data are free of cloud contamination due to pre and post-field calibration (Giles et al., 2019); iii)~~ Second, this study only considered the daytime period (from ~~06:00~~ 07:00 to 17:00 LT) because the highest R_n values occur during this time. After filtering, the resulting dataset is summarized in Table S1 and S2. ~~the database was reduced to 523 rows: 370 in the dry season and 153 in the wet season. Of the filtered data, 2020 had the highest availability at 42.4 %, followed by 2022 at 29.2%, then 2016 at 20 %, 2021 at 4.9 %, 2019 at 3 %, and finally 2017 at 0.5 %, however, no data was available for 2018 (0%). This distribution reflects the difficulty of obtaining robust data sets to assess the effects of aerosols.~~

Using the values for humidity ~~,~~ and temperature ~~and atmospheric pressure~~(variables shown in Table 1), it was possible to calculate the vapor pressure deficit (VPD) ~~and the mixing ratio (r)~~ using Equations 1 ~~and 4~~ to 3 ~~The calculated and directly measured variables in Table 1 allowed the Random Forest model (explained in Section 2.3) to be used to calculate the impact of aerosols on the energy and matter fluxes. VPD was calculated~~ according to ~~the equations used by~~ Bolton (1980).

$$VPD = e_s - e_a \tag{1}$$

The water vapor saturation pressure (e_s) as a function of temperature (T) was calculated according to the equation Tetens (1930).

$$e_s(T) = 6.112exp(\frac{17.67 \cdot T}{T + 243.5}) \tag{2}$$

The actual vapor pressure (e_a) was obtained by relating it to the relative humidity (RH).

$$e_a = RH \cdot e_s \tag{3}$$

~~r was calculated using a process that satisfies the equivalent potential temperature equation, as described by Holton (2013). In this equation, P_{atm} represents the atmospheric pressure.~~

$$r = \frac{622 \cdot e_a}{P_{atm}} - e_a \tag{4}$$

2.3 Analysis methods

~~Initially, daily averages of AOD values were obtained to investigate seasonal variability. The days with extreme AOD values were then selected for which hourly averages were obtained between 06:00 and 17:00 LT. To explore how extreme AOD conditions influence surface turbulent fluxes, a 4th-order polynomial adjustment was used, similar to that carried out by Meyers and Dale (1983).~~

~~This analysis enabled the behavior of the variables to be investigated under two extreme atmospheric conditions: the 'Polluted' and 'Clean' regimes in the ATTO region, which are characterized by high and low aerosol loads ($AOD > 0.40$ and $AOD < 0.13$, respectively).~~

Daily averages of AOD values were obtained to investigate seasonal variability. Our analysis distinguishes two contrasting atmospheric conditions at the ATTO site, defined as "Clean" and "Polluted" using AOD thresholds derived from the dry-season distribution of AOD. The Clean and Polluted regimes correspond to the 10th ($AOD \leq 0.13$) and 90th ($AOD \geq 0.40$) percentiles, respectively. Further details on the seasonal aerosol analysis are provided in Section 3.1 and Table S3. Subsequently, 30-min AOD averages between 07:00 and 17:00 LT were computed to ensure temporal consistency with the surface flux data and enable direct comparisons. To improve the visualization of the mean diurnal patterns, a 4th-order polynomial curve was applied exclusively as a smoothing technique to the observational data. This curve fitting was used solely for graphical purposes and does not represent a physical or predictive model. All analyses were based on the measured data. For comparisons between Clean and Polluted regimes, only the interval from 10:00 to 14:00 local time was considered, as this period corresponds to the maximum net radiation at the study site and minimizes the influence of low solar elevation angles.

Statistical differences in meteorological variables and surface fluxes between the Clean and Polluted regimes were assessed using the Mann-Whitney U test. This non-parametric approach was selected because the observational data violated the assumption of normality, as confirmed by preliminary Shapiro-Wilk tests. The Mann-Whitney U test was used to determine whether the median values of the two independent regimes differed significantly ($p < 0.05$), offering a robust framework for analyzing non-normally distributed atmospheric data (Wilks, 2011).

~~Statistical analyzes were also used: i) Spearman's correlation to assess monotonic relationships between variables; ii) Pillai's trace test to analyze multiple dependent variables (R_n, H, LE and FCO_2) in relation to the independent variable (AOD); iii) Random Forest machine learning to determine aerosol importance in relation to flux variables, generating a model for each flux (R_n, H, LE and FCO_2) as a dependent variable and the variables in Table 1 as independent variables.~~

~~Pillai (1955) developed equation 5, which is widely used in analyses such as multivariate analysis of covariance (MANCOVA), particularly when assumptions are violated, such as when the covariance matrices are inhomogeneous.~~

$$p(T^{(s)}) = \frac{(T^{(s)})^{sm}}{(1+T^{(s)})^{s(2m+2n+s+1)/(2+1)}\beta[sm+1, \frac{1}{2}s(2n+s+1)]}, 0 < T^{(s)} < \infty \quad (5)$$

~~Where, 'm' and 'n' are related to the sample sizes, 's' is a rank defined by the sum of the products of the matrix, 'p' are the characteristic roots of the matrix with values ranging from 0 to 1, 'T' summarizes the magnitude of the difference between the groups in relation to all dependent variables and 'β' is used to calculate the p-value associated with the Pillai trace statistic.~~

~~A p($T^{(s)}$) value close to zero indicates that there is greater overlap between categorical groups in a multivariate space. A p-value below 5 % indicates that there is statistical significance between the dependent variables in relation to the categorical groups.~~

~~Finally, the importance of aerosols in relation to flux variables was determined using the Random Forest machine learning algorithm. According to Biau and Scornet (2016), this method provides accurate and reliable predictions because it combines multiple decision trees, thus minimizing the risk of overfitting — when the model fits the training data too well, compromising its ability to generalize. The algorithm follows the 'divide and conquer' principle by sampling fractions of the data, building randomized tree predictors for each subset, and aggregating the results.~~

~~The estimation of the finite nonparametric regression forest presents the combination of decision trees by Equation 6 (Biau and Scornet, 2016).~~

$$\hat{m}_{M,n}(x; \Theta_1, \ldots, \Theta_M, D_n) = \frac{1}{M}\sum_{j=1}^{M} m_n(x; \Theta_j, D_n) \quad (6)$$

~~Where: $\hat{m}$ is the prediction of the model for an observation x; M is the number of random regression trees; n is the number of observations in the training set D_n; the values $\Theta_1, \ldots, \Theta_M$ are independent random variables associated with each tree j; and the predicted value at the query point x is denoted by $m_n(x; \Theta_j, D_n)$.~~

~~Thus, the Random Forest is an ensemble method that combines several decision trees (M trees), where each tree (j) makes a prediction $m_n(x; \Theta_j, D_n)$ for observation x, arriving at an average of the predictions of all trees.~~

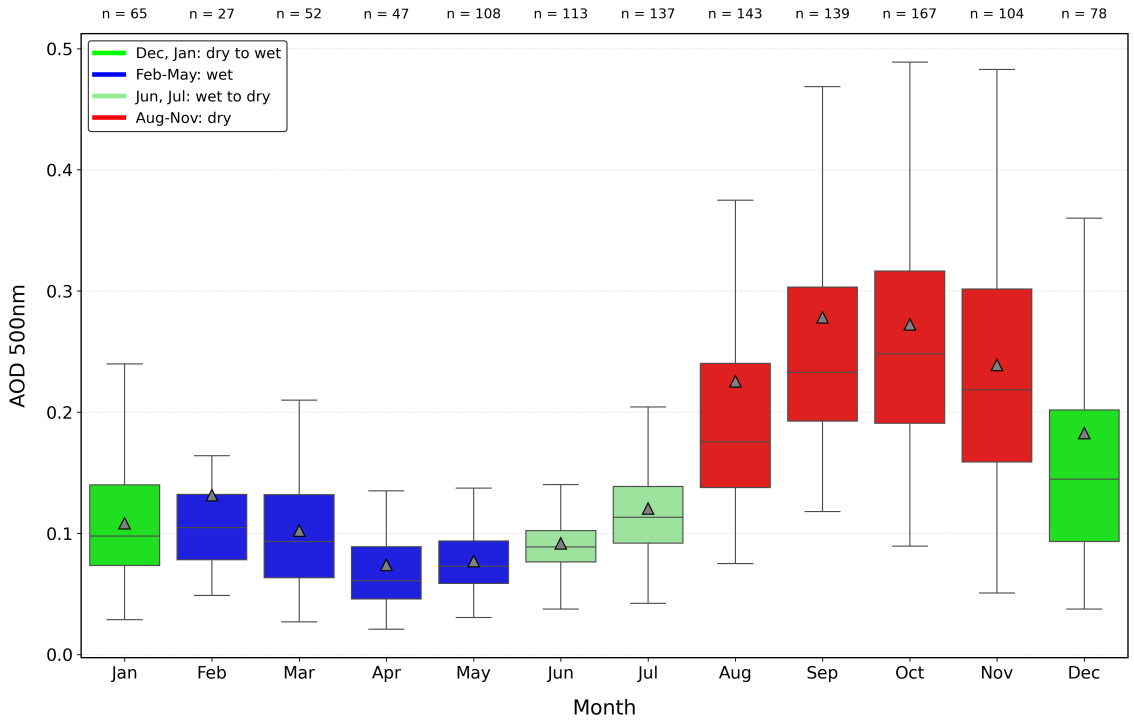

Figure 2. Box plot showing monthly AOD 500 nm values measured at the ATTO site between 2016 and 2022. The box represents the central 50 % of the data, the whiskers represent the smallest and largest non-outlier values, while the means are indicated by the green triangles and the medians are the lines inside the box. Numbers above each month indicate the sample size (n).

3 Results and Discussion

3.1 Characteristics of seasonal aerosol variation

The distribution of atmospheric aerosols, expressed as AOD, exhibits a clear seasonal cycle at the ATTO site (Figure 2). The lowest values occur during the wet season, with an average of 0.07 in April, while the dry season is marked by higher AOD values, reaching an average of 0.28 in September. Furthermore, this seasonal variation in AOD values has previously been observed at other sites in the Amazon region (Artaxo et al., 2013; Cirino et al., 2014; Morais et al., 2022; Palácios et al., 2022). Cirino et al. (2014), for example, used data measured at the ZF2 site, located 60 km northwest of Manaus in central Amazonia, to show that AOD values were close to 0.4 (with peaks above 0.5) in the dry season and less than 0.2 in the wet season. Attention is drawn to the AOD values observed in the southern region of the Amazon basin, which is influenced by the arc of deforestation, an agricultural frontier zone with intense burning activity during the dry season (Davidson et al., 2012). Several studies in this region have shown that AOD values often exceed 4 in the dry season, whereas in the wet season they rarely exceed 0.2 (Fuzzi et al., 2007; Artaxo et al., 2013; Palácios et al., 2024).

The main distinction between the AOD values measured ~~above~~ at the ATTO site and those measured in the southern Amazon is the magnitude of these values. In particular, the AOD values at the ATTO site are approximately 15 times lower than those in the region close to the arc of deforestation during the dry season (Sena et al., 2013; Palácios et al., 2020). ~~Andreae et al. (2015),~~ Pöhlker et al. (2018) and Holanda et al. (2023) for example, investigated the seasonal contrast of aerosols at the ATTO site, highlighting that parts of the wet season resemble preindustrial conditions with minimal human impact.

Figure 3 shows the average daily AOD values for the dry and wet seasons, from 2016 to 2022. It is clear to see that the highest average AOD values were obtained during the dry season, with values ~~exceeding~~ reaching 1.5, while in the wet season these values did not exceed 0.5, a result similar to that already reported in Figure 2. It should also be noted that during the dry season, the 90th and 10th percentiles of the AOD values are 0.40 and 0.13, respectively. During the wet season, these percentiles were 0.13 and 0.04, respectively. In other words, the AOD values above the 90th percentile in the wet season are slightly higher than the values observed for the 10th percentile in the dry season. This reinforces what was already mentioned in Figure 2, that the wet season in the ATTO region is quite 'Clean' compared to the dry season. ~~As the main goal of this work is to investigate the impact of the presence of aerosols on surface turbulent fluxes, from now on we will only work with data from the dry season, and for this we will use two classes: i) "Clean regime" being the one in which the AOD values were below the 10th percentile, and ii) "Polluted regime" being the one in which the AOD values were above the 90th percentile.~~ As the main goal of this work is to investigate the impact of aerosols on surface turbulent fluxes, the analysis focuses on data from the dry season. In addition, during the dry season there is more aerosol data since the could interference is much less pronounced than during the wet season. Two aerosol regimes were defined based on percentile thresholds of the dry-season AOD distribution. Several percentile combinations were tested to assess the robustness of the regime separation. Based on this analysis, the 10th and 90th percentiles were selected to define the Clean ($AOD \leq 0.13$) and Polluted ($AOD \geq 0.40$) regimes, respectively, as they preserve physically meaningful differences between aerosol regimes (See Table S1).

3.2 Relationship between AOD and surface turbulent fluxes

As described in Section 2.3, the comparisons between Clean and Polluted regimes were restricted to the 10:00–14:00 LT period, corresponding to the maximum net radiation. The full diurnal cycles of shortwave, longwave, and net radiation during the dry season (2016–2022) show that the maximum values occur between 10:00 and 14:00 LT (Figure 4), supporting the choice of this time window for the subsequent analyses. The average values of the radiation balance components during ~~the~~ this period ~~of greatest radiative and convective activity between 10:00 and 14:00 LT in the ATTO are shown~~ are summarized in Table 2. The negative sign in the difference between the Polluted and Clean regimes indicates that the radiative components decrease during this period. The R_{n} fell the most in relative terms, by around ~~-6~~ -4 %. Outgoing shortwave radiation (SW_{out}) ~~was the least affected by pollution, with a decrease of just -0.16.~~ showed a non-significant increase of 3.3% (p = 0.07). As is well known, the longwave balance is always negative during the daytime in the Amazon region (von Randow et al., 2004) since LW_{terr} is greater than LW_{atm}. However, pollution reduced the difference between LW_{atm} and LW_{terr} by around ~~8~~ 2 Wm^{-2} compared to the Clean regime, indicating a slightly less radiative surface and a slightly warmer atmosphere.

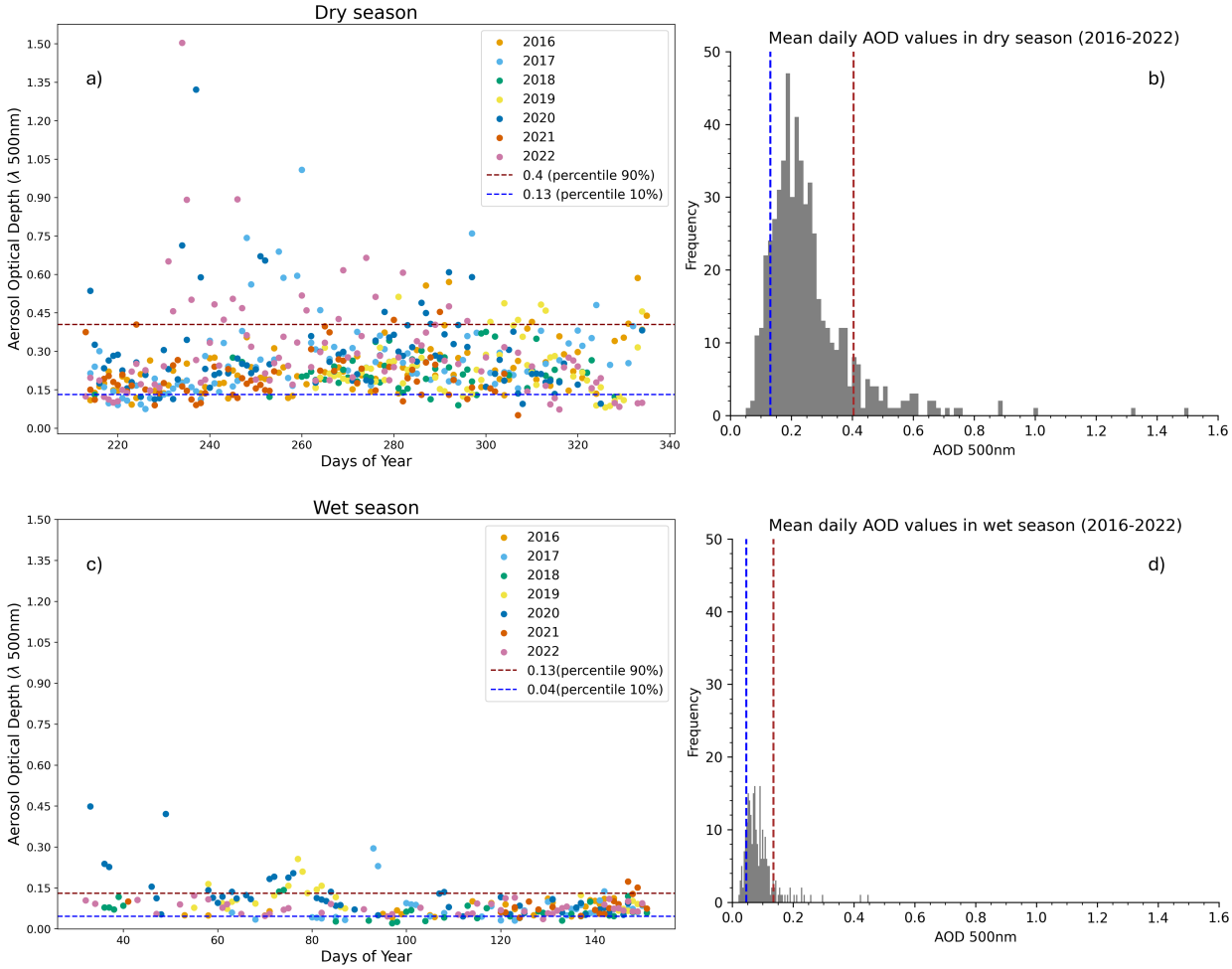

Figure 3. (a) and (c) Daily AOD averages (500 nm), (b) and (d) their respective histograms. Values above the red line indicate high aerosol concentration (above the 90$^{\text{th}}$ percentile), while values below the blue line indicate low aerosol concentration (below the 10$^{\text{th}}$ percentile).

Quantifying the impact of aerosols on radiative flux remains a significant challenge in climate system studies, with persistent uncertainties (Palácios et al., 2022). However, the relationship between aerosols and radiative flux has been investigated for decades in the Amazon region (Ross et al., 1998; Procopio et al., 2004; Rizzo et al., 2011; Artaxo et al., 2013; Palácios et al., 2022). There is a consensus in the literature that an increase in AOD reduces SW_{in}, which consequently also causes a reduction in R_{n}. However, the magnitude of these reductions varies considerably. Studies carried out during the dry season in the Amazon rainforest using different methods to estimate direct aerosol radiative forcing (ARF) illustrate this variability. For example, Ross et al. (1998) reported an average daily ARF of -20 $\pm$ 7 Wm^{-2} per unit of AOD at 550 nm in the Amazon rainforest. ~~In contrast,~~ Consistent with these findings, Palácios et al. (2022) estimated an average ARF of -20.77 $\pm$ 5.04 Wm^{-2} for the dry season in the central Amazon. Procopio et al. (2004) found daily ARF values ~~(ARF24h)~~ ranging from -21 to -74

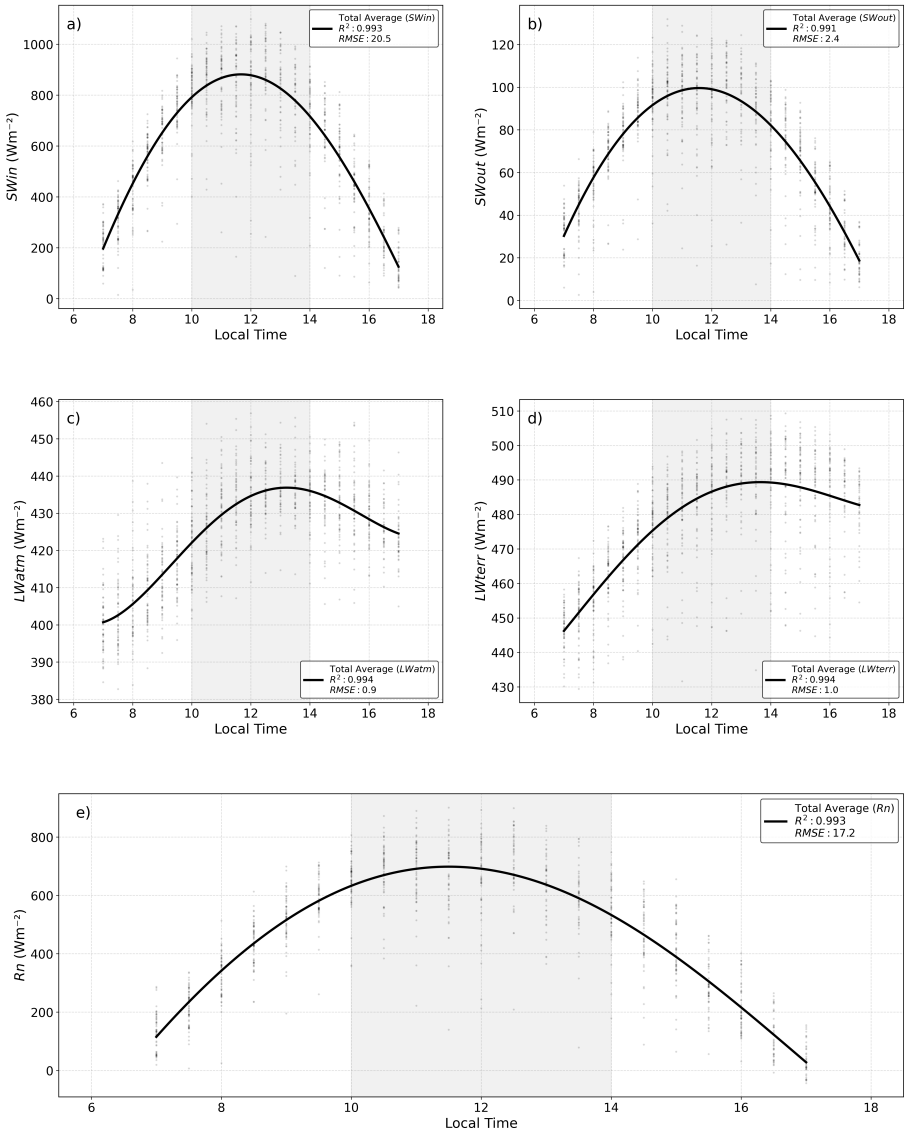

Figure 4. Diurnal cycles of radiative fluxes during the dry season from 2016 to 2022: (a) incoming ($\mathrm{SW_{in}}$) and (b) outgoing ($\mathrm{SW_{out}}$) shortwave radiation, (c) incoming atmospheric ($\mathrm{LW_{atm}}$) and (d) outgoing terrestrial ($\mathrm{LW_{terr}}$) longwave radiation, and (e) net radiation (R_n). Markers indicate observed data, and solid lines represent fourth-order polynomial fits, with the corresponding $\mathrm{R^2}$ and RMSE

$\mathrm{Wm^{-2}}$ in the deforestation arc, an area with higher levels of pollution than the central Amazon. Rizzo et al. (2011) investigated this central region and reported ~~an ARF24h~~ a daily ARF value of -32 $\mathrm{Wm^{-2}}$.

230 Although these studies provide estimates of the reduction in surface radiation from aerosols in the Amazon, they do not converge on a single consensus value. This is because, in addition to the different methodologies used to obtain ARF values, Procopio et al. (2004), Sena et al. (2013) and Palácios et al. (2020, 2022) point out that uncertainties lie mainly in the

Table 2. Averages of the radiation components in the period from 10:00 to 14:00 LT, during the dry season from 2016 to 2022, with the respective relative difference between the Polluted and Clean regimes.

Means of radiation variables			
Variables	Polluted	Clean	Relative Difference
SWin ($\mathrm{W\,m^{-2}}$)	~~797.61 ±129.33~~813.5 ±124.4	~~844.81 ±145.27~~836.5 ±165.2	~~-5.59~~-2.8
SWout ($\mathrm{W\,m^{-2}}$)	~~94.79 ±14.67~~95.9 ±15.1	~~94.94 ±16.70~~92.8 ±19.7	~~-0.16~~3.3
LWatm ($\mathrm{W\,m^{-2}}$)	~~431.99 ±9.61~~432.1 ±9.4	~~428.11 ±10.14~~431.5 ±10.4	~~0.90~~0.1
LWterr ($\mathrm{W\,m^{-2}}$)	~~483.61 ±8.95~~483.6 ±10.8	~~487.67 ±11.32~~484.7 ±14.0	~~-0.83~~-0.2
R_n($\mathrm{W\,m^{-2}}$)	~~617.33 ±103.72~~632.8 ±100.8	~~656.98 ±117.59~~659.3 ±137.8	~~-6.04~~-4.0

complex interactions between types and concentrations of aerosols, surface characteristics, atmospheric conditions, and solar ~~geometry~~angle.

SW_{out} is directly related to surface albedo and the fact that it did not change significantly in our data between regimes (maintaining albedo at ~ 0.11) indicates that pollution has a secondary effect compared to the characteristics of the surface itself. There is a wide range of surface characteristics in the Amazon that directly influence albedo, as observed by von Randow et al. (2004) and Pareja-Quispe et al. (2021): i) degree of vegetation cover; ii) soil and vegetation water conditions; iii) solar elevation; iv) cloud cover and; v) wind speed and direction.

However, the behavior of longwave radiation was quite interesting. It shows that because of their interaction with the incident shortwaves, aerosols increase the emission of thermal energy toward the surface. At the same time, they act as a barrier to the total energy reaching the surface, thus impacting the amount of thermal energy emitted by the surface itself. The increase in LW_{atm} and the decrease in LW_{terr} in the Polluted regime result in a smaller longwave balance in this regime. de Menezes Neto et al. (2016) also observed this effect in their experiments involving biomass burning aerosols in South America: a subtle variation in longwave intensity attributed to the presence of aerosols.

With reduced solar energy input on the surface during the Polluted regime, cooling occurs at the forest-atmosphere interface, accompanied by a decrease in VPD compared to the Clean regime, as illustrated in Figure 5. The cooling between the 10:00 and 14:00 LT regimes implies an average ~~temperature~~ reduction ~~on the canopy surface of 0.53 °C~~ in canopy surface temperature of 0.9 °C, based on infrared surface temperature measurements, and a corresponding reduction in air temperature of 0.3 °C, resulting in a ~~-3.21~~ -2 hPa (~~19.5~~ 13%) decrease in VPD.

As the curve for the Clean regime is consistently above that for the Polluted regime at all shown temperatures, it is suggested that the Clean regime will first achieve a reduction in evapotranspiration, given the approximately linear relationship between temperature and VPD.

These cooling values are consistent with the effects documented in other studies. For example, Moreira et al. (2017) found a reduction in 1.2 °C above the Amazon region, while Cirino et al. (2014) identified a 1.8 °C and a decrease in 35% in VPD in the central Amazon. In the deforestation arc, Rodrigues et al. (2024) found an average cooling effect of between 3 °C and 4 °C, as well as reductions of between -2 and -3 hPa in VPD.

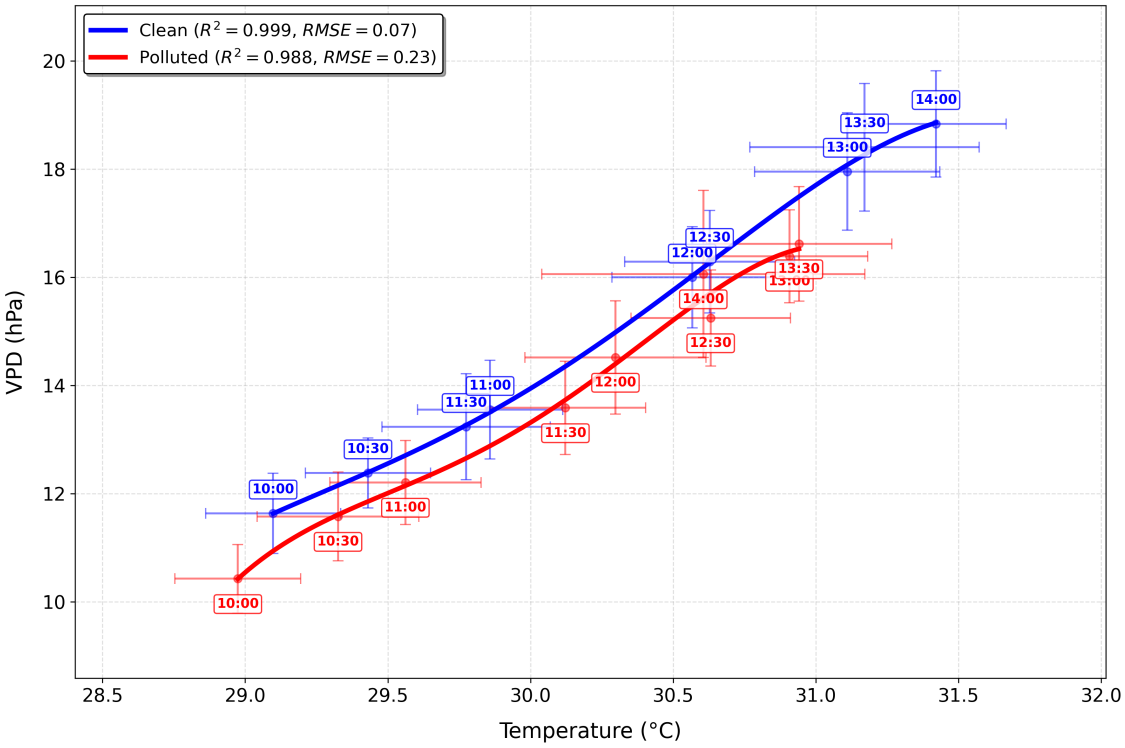

Figure 5. Relationship between temperature and vapor pressure deficit (VPD) above the forest canopy at the ATTO for ~~the different regimes (Clean and Polluted)~~ Clean and Polluted regimes during the dry season (2016-2022).

Braghiere et al. (2020) investigated temperature variations in the Amazon using a radiative transfer model. By simulating a scenario without aerosols (AOD = 0) and comparing it with real conditions, they observed an increase in temperature in the scenario without aerosols. They identified a correlation between relative irradiance, air temperature, and VPD. Meanwhile, Herbert and Stier (2023) and Palácios et al. (2024) reinforce the idea that AOD significantly influences temperature variations, particularly on a regional scale. For instance, Palácios et al. (2024) observed positive linear correlations between AOD and air temperature across distinct climatic phases, attributed to the absorption of solar radiation by biomass burning emissions resulting in atmospheric heating. Similarly, Herbert and Stier (2023) utilized reanalysis data to demonstrate that 2-meter air temperature increases as a function of AOD, consistent with localized heating of the smoke layer due to strong absorption of solar radiation.

Herbert and Stier (2023) and Palácios et al. (2024) also highlight that the physical characteristics of the aerosols present in the atmosphere, such as size, mixing state and presence of coatings, as well as the chemical characteristics, such as the ability to absorb or scatter light and hygroscopicity, determine their direct impact on temperature and VPD through radiative interaction, as well as their indirect impact by influencing cloud properties and evapotranspiration rates. These are essential components of the atmosphere's energy balance.

The interaction between aerosols, radiation, and evapotranspiration affects not only temperature and VPD, but also the fluxes of energy and matter on the surface. This has a direct impact on atmospheric and ecosystem processes. Figure 6 illustrates the impact of aerosols on these fluxes. ~~It can clearly be seen~~It shows that for the Polluted regime, the values were lower than those observed during the Clean regime, especially during periods of high solar radiation, i.e. between 10:00 and 14:00 LT. ~~As previously mentioned, the~~The most significant reductions in the energy available to the surface occur during this period, with R_n falling by ~~-6~~ -4%, as reflected in the energy partitions. The surface energy balance closure was 0.89 for the Clean regime and 0.88 for the Polluted regime, comparable to values reported in the literature (Mauder et al., 2024). The corresponding residuals were of similar magnitude (70 $\mathrm{Wm^{-2}}$ for Clean and 75 $\mathrm{Wm^{-2}}$ for Polluted), indicating that the observed differences in energy fluxes are not related to differences in energy balance closure.

Sensible heat decreased by an average of ~~-17.30~~ -21.7 $\mathrm{Wm^{-2}}$ (~~11.3~~13.5%), reflecting reduced energy transfer to the atmospheric boundary layer. Similarly, LE decreased by ~~-45.08~~ -8.9 $\mathrm{Wm^{-2}}$ (~~10.4~~2%), indicating limited evapotranspiration due to the reduced radiative energy available. The Bowen ratio, which relates H and LE, ~~remained at 0.35 for both regimes,~~ recorded 0.38 in the Clean regime and 0.33 in the Polluted regime, suggesting that a higher proportion of energy was allocated to latent processes, as expected in forest environments. ~~The sum of H and LE was also found to be 67.85 $\mathrm{Wm^{-2}}$ lower for the Clean regime than for R_n, while for the Polluted regime, this value was 91.18 $\mathrm{Wm^{-2}}$. It appears that the Polluted regime is further from the energy balance close, suggesting a change in how this energy is distributed.~~ The ground heat flux (G) also decreased by ~~-0.60~~ -1.0 $\mathrm{Wm^{-2}}$ (~~39.3~~ 54.5%), demonstrating its greater sensitivity to variations in R_n compared to turbulent fluxes.

In addition to their effect on energy fluxes, aerosols were found to have a significant influence on ~~flux CO_2, showing an average drop~~ CO_2 flux, becoming more negative by an average of ~~5.69~~ 4.9 $\mu\mathrm{mol\,m^{-2}\,s^{-1}}$ (~~57.7~~ 39.5%) in the Polluted regime compared to Clean conditions between 10:00 and 14:00 LT. This is when the difference between the Polluted and Clean regimes is most pronounced, indicating that the forest absorbs more CO_2 in the Polluted regime (Figure 7). The reductions in H, LE, G, and FCO_2 shown in Figure 6 and Figure 7 were also observed across individual years (see Fig. S3).

In the Polluted regime, ~~an increase in gas exchange due to photosynthesis is visible in Figure 7, suggesting a possible increase in evapotranspiration.~~ CO_2 fluxes were more negative (Figure 7), indicating increased CO_2 uptake by vegetation related to photosynthetic activity. Such enhanced photosynthesis may be linked to changes in stomatal regulation that allow greater CO_2 uptake without a proportional increase in transpiration, reflecting higher stomatal conductance efficiency (Liu et al., 2022; Crous et al., 2025). However, analysis of the ~~energy available for evapotranspiration (LE)~~ LE, which represents the fraction of available energy converted into evapotranspiration, shows a consistent decrease in the Polluted regime compared to the Clean regime (Figure 6)~~, which contradicts this expectation.~~

The apparent paradox of an increase in CO_2 absorption alongside a reduction in LE can be explained by water use efficiency (WUE). According to Dekker et al. (2016) and Yang et al. (2016), WUE is defined as the ratio of carbon assimilated to water transpired by vegetation. In this study, WUE was estimated using FCO_2/LE as a proxy. WUE was significantly higher under Polluted compared to Clean regime (mean values of 0.042 and 0.029, respectively, $p < 0.05$). This indicates that, under Polluted regimes, vegetation assimilates more carbon per unit of water lost, consistent with the observed reduction in latent heat flux Figure 6 despite enhanced CO_2 uptake Figure 7. ~~Studies in the Amazon indicate that higher temperatures and consequently~~

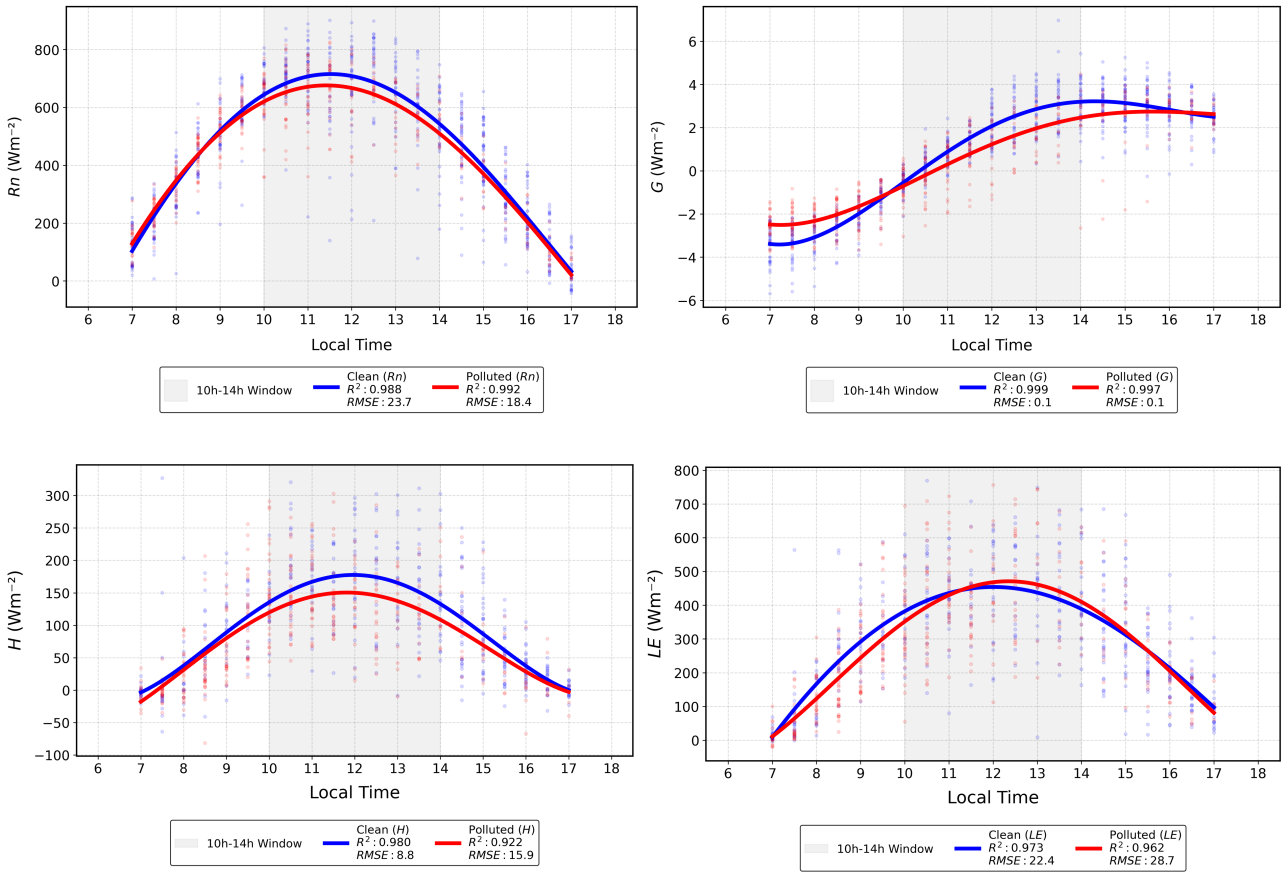

Figure 6. Diurnal cycle of surface fluxes ~~in~~ during the dry season (2016-2022)~~, with emphasis on the time between 10:00 and 14:00 LT. In blue are the curves with data from days in the Clean regime, in red the data from days in the Polluted regime and in green the respective difference between the variables.~~ under Clean (blue) and Polluted (red) regimes, highlighting the 10:00–14:00 LT period. R_n (net radiation), G (ground heat flux), H (sensible heat flux), and LE (latent heat flux).

~~higher VPD generally result in lower WUE (Aguilos et al., 2018; Botía et al., 2021). Our results (Figure 5) show that, at peak solar radiation (12:00 LT), temperatures of 30.5 °C and 31.2 °C and VPD values of 14.2 and 18.0 were observed in Polluted and Clean regimes, respectively. These values suggest a higher efficiency in carbon assimilation in the Polluted regime, as shown in Figure 7, and less water is emitted by evapotranspiration, as shown in Figure 6, with fewer LE assigned to this process.~~

In forests in the USA, Steiner et al. (2013) conducted experiments to quantify the impact of aerosols on turbulent surface fluxes, observing reductions in H and LE ranging from 10% to 30%. Few studies have examined the relationship between H, LE and AOD in the Amazon region. Zhang et al. (2008), for example, used regional modeling with an AOD threshold of 0.3 to obtain a daily average reduction of -15 Wm^{-2} for H and -5 Wm^{-2} for LE. In the deforestation zone, Braghiere et al.

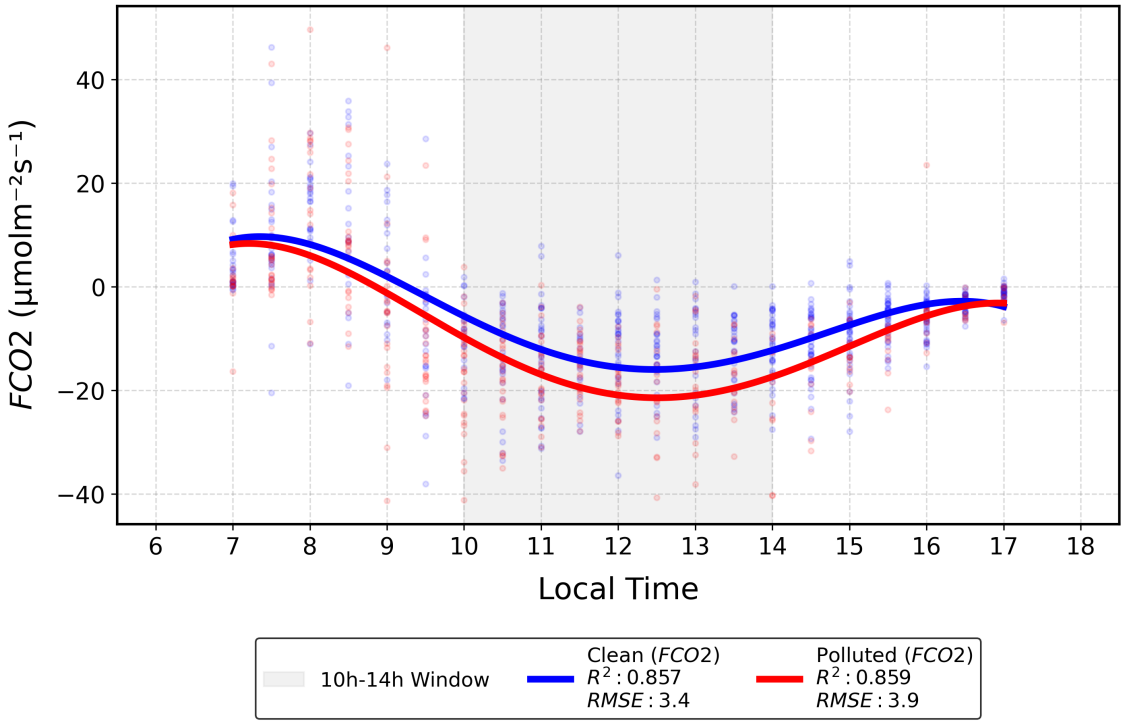

Figure 7. Diurnal cycle of CO_2 flux (FCO_2) during the dry season (2016–2022) under Clean (blue) and Polluted (red) regimes, highlighting the 10:00–14:00 LT period. ~~The diurnal cycle of matter flux in the ATTO region between 06:00 and 17:00 LT, fitted with a fourth-order polynomial. The data are from the dry season between 2016 and 2022, with emphasis on the period between 10:00 and 14:00 LT. The blue curves show the data from days in the Clean regime, the red curves show the data from days in the Polluted regime, and the green curves show the difference between the two.~~

(2020) observed a decrease of -67 Wm^{-2} (36%) for H and -4 Wm^{-2} (2%) for LE when simulating Clean conditions (AOD = 0) and comparing them with real conditions involving the presence of aerosols. These results suggest that regional climate models may underestimate the reduction in LE, highlighting the importance of biological processes, such as transpiration, in compensating for these effects.

In contrast, numerous studies in the Amazon have demonstrated the significant impact of aerosols on CO_2 assimilation by forests. This occurs by increasing the diffuse fraction of photosynthetically active radiation reaching forest shade zones, thereby intensifying photosynthesis. Simultaneously, it reduces the net direct solar radiation reaching the canopy surface, thereby generating photosynthetic enhancement in this region (Doughty et al., 2010; Cirino et al., 2014; Rap et al., 2015; Moreira et al., 2017; Malavelle et al., 2019; Rodrigues et al., 2024). This diffuse fraction, which falls within the wavelengths of interest for vegetation (0.4 to 0.7 μm), can increase from around 19% (the typical value of a Clean atmosphere) to 80% under biomass burning conditions (Yamasoe et al., 2006).

Table 3. Influence of aerosols on surface turbulent fluxes, considering all 370 runs of data (see section 2.2), from 06:00 to 17:00 LT, at 30-minute average intervals. The MSE of H and FCO_2 was obtained by cross-validation, a technique applied to improve the accuracy of the model due to less adjusted initial values. The MSE for R_n and LE did not require cross-validation, as they already showed an adequate fit.

The influence of aerosols on energy and matter fluxes

Model	AOD	MSE	R^2
R_n	0.027	0.19	0.81
H	0.030	0.30	0.65
LE	0.032	0.28	0.74
FCO_2	0.066	0.38	0.46

We quantified the diffuse radiation fraction ($F_d = SW_d/SW_{in}$) for the available period (2021) and compared F_d between Clean and Polluted aerosol regimes. Our results indicate higher F_d values under Polluted regime compared to Clean regime (Figure S1). Specifically for the 10:00 and 14:00 LT interval, the mean F_d values were 0.43 and 0.27 for Polluted and Clean regime, respectively, indicating an absolute difference of 0.16 between the two regimes ($p<0.05$). This is consistent with enhanced scattering of solar radiation associated with increased aerosol loading (Giorgi et al., 2002; Seinfeld and Pandis, 2016; Ezhova et al., 2018). Moreover, daytime CO_2 fluxes showed a non-linear dependence on F_d, with net CO_2 uptake increasing up to an F_d threshold (≈ 0.6) and decreasing at higher F_d values (Figure S2). This behaviour was consistent with the response of net ecosystem exchange for diffuse radiation reported by Deng et al. (2022) for four forest sites in China and aligns with the global-scale mechanisms proposed by Mercado et al. (2009). These results provide observational support for the proposed mechanism linking aerosol loading, radiation partitioning, and ecosystem carbon exchange.

3.3 Influence of aerosols on surface turbulent fluxes

The statistical correlations between aerosols and surface turbulent fluxes reveal monotonic relationships of low intensity or with no statistical significance. Furthermore, MANCOVA analysis with Pillai trace indicated a highly significant multivariate effect ($p < 0.001$). These findings suggest that the impact of aerosols on fluxes cannot be fully explained by linear relationships alone, but rather by nonlinear interactions with other environmental factors such as temperature, humidity and wind.

Table 3 shows the relative contribution of AOD to the prediction of each flux model value, as obtained using the Random Forest machine learning (RFM) technique and the variables in Table 1. This was done to capture the nonlinear influence between aerosols and surface turbulent fluxes.

The results of the RFM (see Table 3) suggest that R_n performed best in terms of predictive capacity, with an R^2 of 0.81 and an MSE of 0.19. In contrast, FCO_2 performed the worst, with an R^2 of 0.46 and an MSE of 0.38. The lower value R^2 for FCO_2 can be attributed to the greater complexity of the interactions between aerosols and the biophysical processes that regulate this flux. However, AOD had a significantly greater impact on the predictive performance of FCO_2 (6.6%), which is more than double the values observed in the energy fluxes (LE: 3.2 %; H: 3.0 %; R_n: 2.7 %), R_n showing the least influence of all the energy fluxes.

~~These results corroborate the analyses in Section 3.2, which examined the period of the greatest radiative and convective activity and identified significant reductions in fluxes under the influence of AOD. The most significant reduction was recorded for FCO_2 -57.7%), followed by a balance between H (-11.3%) and LE (-10.4 %), while the smallest reduction was observed for R_n (-6 %).~~

~~In summary, these findings demonstrate that aerosols influence surface fluxes in a complex, nonlinear manner, with varying impacts depending on the type of flux analyzed. FCO_2 shows greater sensitivity, reflecting intricate biophysical processes, while energy fluxes respond more moderately, being more closely linked to the impact of these aerosols on energy partitioning.~~

4 Conclusions

This study assessed, for the first time, the impact of aerosol regimes on the exchange of surface energy (net radiation - R_n, sensible heat - H and latent heat - LE) and mass (carbon dioxide flux - FCO_2) at the forest-atmosphere interface in the central Amazon, a region that experiences relatively pristine atmospheric conditions during part of the year. Based on long-term data collected between 2016 and 2022 at the ATTO site, our analysis provides clear and quantitative evidence that high aerosol loads ($AOD > 0.40$) reduced the magnitude of FCO_2, H, and LE fluxes compared to Clean conditions ($AOD < 0.13$).

During the peak radiation period (10:00-14:00 LT), the Polluted regime ($AOD > 0.40$) substantially reduces turbulent energy fluxes, decreasing H by ~~17.3~~ 21.7 Wm^2 (~~11.3~~ 13.5%) and LE by ~~45.08~~ 8.9 Wm^2 (~~10.4~~ 2.1%). Simultaneously, the forest's net CO_2 absorption increased, with FCO_2 decreasing by ~~-5.69~~ -4.9 $\mu mol\, m^{-2}\, s^{-1}$ (~~57.7~~ 39.5%), indicating a significant increase in carbon assimilation. This biophysical response was accompanied by a cooling of the forest-atmosphere interface by ~~0.53~~ 0.9°C and a reduction in the vapor pressure deficit (VPD) by ~~3.21~~ 2.0 hPa (~~19.5~~ 12.9%). Thus, aerosols also play an important role in modulating energy partitioning ~~and gross primary productivity~~ in the tropical forest ecosystem.

Our findings indicate that even in the relatively pristine central Amazon during the dry season, a threshold aerosol load (AOD 0.40) exists, above which significant impacts on energy fluxes occur. This suggests that in regions with higher aerosol loads, such as the southern Amazon's arc of deforestation, impacts on energy balance could be even more severe.

Our statistical analyses indicate that aerosols and surface turbulent fluxes interactions are predominantly indirect and non-linear, mediated by environmental variables like radiation, temperature, and humidity. Consequently, different inflection points likely exist across the Amazon, and the AOD threshold identified here cannot be applied to the entire region. Furthermore, isolating the aerosol effect from clouds requires rigorous filtering and a significant data collection effort, as cloud-free moments are scarce in long-term Amazonian time series.

Our work advances knowledge by quantifying the simultaneous effects of ~~aerossol~~ aerosol on energy and matter fluxes, bringing with it possibilities for improvements in climate models for the Amazon region and opening up the possibility of future work aimed at coupling the carbon and water cycles, mediated by aerosols, shedding light on the functioning of forest ecosystems. All of this is possible with the integrated analysis of diffuse radiation and the efficient use of water combined with the impact of aerosols on energy and matter fluxes.

In addition, future work involving remote sensing and data from micrometeorological towers throughout the Amazon is crucial in order to spatialize the results of all these dynamics between the forest-atmosphere interface, which is essential for quantifying the impact of aerosols on the Amazonian climate system.

Author contributions. Conceptualization: MABdR, CQDJ, JCPCand FAFDO. Data curation: CQDJ, ACdA, CP, SR and PA. Formal analysis: MABdR, CQDJ. Funding acquisition: CQDJ. Investigation: MABdR, CQDJ and FAFDO. Methodology: MABdR, CQDJ, FAFDO and RSP. Project administration: CAQ, CQDJ. Resources: CQDJ, ACdA, CP, SR and PA. Software: MABdR and FAFDO. Supervision: CQDJ and RSP. Validation: MABdR and FAFDO. Writing (original draft preparation): MABdR, CQDJ. Writing (review and editing): MABdR, CQDJ, JCPC, FAFDO, ACSM, CP, SR, ACdA, MAF, PA, CAQ, RSP.

Competing interests. The authors declare that they have no conflict of interest.

Acknowledgements. Mariano A.B. da Rocha thanks the Coordenação de Aperfeiçoamento de Pessoal de Nível Superior - Brasil (CAPES) for the PhD grant awarded through the Environmental Science Graduate Program (PPGCA/UFPA). Cléo Q. Dias-Júnior acknowledges support from CNPQ (Processes 406884/2022-6, 307530/2022-1, 406307/2023-7, 444929/2024-0, 445451/2024-6 and 404254/2024-1). This study is part of the Amazon Tall Tower Observatory (ATTO), funded by the German Federal Ministry of Education and Research (BMBF, contracts 01LB1001A and 01LK1602A), the Brazilian Ministry of Science, Technology and Innovation (MCTI/FINEP, contract 01.11.01248.00) and the Max Planck Society (MPG). ATTO is also supported by the Fundação de Amparo à Pesquisa do Estado do Amazonas (FAPEAM), Fundação de Amparo à Pesquisa do Estado de São Paulo (FAPESP), Universidade do Estado do Amazonas (UEA), Instituto Nacional de Pesquisas Amazônia (INPA), Programa de Grande Escala da Biosfera-Atmosfera na Amazônia (LBA) and the SDS/CEUC/RDS-Uatumã.

References

Aguilos, M., Stahl, C., Burban, B., Hérault, B., Courtois, E., Coste, S., Wagner, F., Ziegler, C., Takagi, K., and Bonal, D.: Interannual and Seasonal Variations in Ecosystem Transpiration and Water Use Efficiency in a Tropical Rainforest, Forests, 10, 14, https://doi.org/10.3390/f10010014, 2018.

Andreae, M. O., Rosenfeld, D., Artaxo, P., Costa, A. A., Frank, G. P., Longo, K. M., and Silva-Dias, M. A. F.: Smoking Rain Clouds over the Amazon, Science, 303, 1337–1342, https://doi.org/10.1126/science.1092779, 2004.

Andreae, M. O., Acevedo, O. C., Araùjo, A., Artaxo, P., Barbosa, C. G. G., Barbosa, H. M. J., Brito, J., Carbone, S., Chi, X., Cintra, B. B. L., da Silva, N. F., Dias, N. L., Dias-Júnior, C. Q., Ditas, F., Ditz, R., Godoi, A. F. L., Godoi, R. H. M., Heimann, M., Hoffmann, T., Kesselmeier, J., Könemann, T., Krüger, M. L., Lavric, J. V., Manzi, A. O., Lopes, A. P., Martins, D. L., Mikhailov, E. F., Moran-Zuloaga, D., Nelson, B. W., Nölscher, A. C., Santos Nogueira, D., Piedade, M. T. F., Pöhlker, C., Pöschl, U., Quesada, C. A., Rizzo, L. V., Ro, C.-U., Ruckteschler, N., Sá, L. D. A., de Oliveira Sá, M., Sales, C. B., dos Santos, R. M. N., Saturno, J., Schöngart, J., Sörgel, M., de Souza, C. M., de Souza, R. A. F., Su, H., Targhetta, N., Tóta, J., Trebs, I., Trumbore, S., van Eijck, A., Walter, D., Wang, Z., Weber, B., Williams, J., Winderlich, J., Wittmann, F., Wolff, S., and Yáñez-Serrano, A. M.: The Amazon Tall Tower Observatory (ATTO): overview of pilot measurements on ecosystem ecology, meteorology, trace gases, and aerosols, Atmospheric Chemistry and Physics, 15, 10 723–10 776, https://doi.org/10.5194/acp-15-10723-2015, 2015.

Artaxo, P. and Orsini, C.: PIXE and receptor models applied to remote aerosol source apportionment in Brazil, Nuclear Instruments and Methods in Physics Research Section B: Beam Interactions with Materials and Atoms, 22, 259–263, https://doi.org/10.1016/0168-583X(87)90339-9, 1987.

Artaxo, P., Rizzo, L. V., Brito, J. F., Barbosa, H. M. J., Arana, A., Sena, E. T., Cirino, G. G., Bastos, W., Martin, S. T., and Andreae, M. O.: Atmospheric aerosols in Amazonia and land use change: from natural biogenic to biomass burning conditions, Faraday Discussions, 165, 203, https://doi.org/10.1039/c3fd00052d, 2013.

Artaxo, P., Hansson, H.-C., Andreae, M. O., Bäck, J., Alves, E. G., Barbosa, H. M. J., Bender, F., Bourtsoukidis, E., Carbone, S., Chi, J., Decesari, S., Després, V. R., Ditas, F., Ezhova, E., Fuzzi, S., Hasselquist, N. J., Heintzenberg, J., Holanda, B. A., Guenther, A., Hakola, H., Heikkinen, L., Kerminen, V.-M., Kontkanen, J., Krejci, R., Kulmala, M., Lavric, J. V., De Leeuw, G., Lehtipalo, K., Machado, L. A. T., McFiggans, G., Franco, M. A. M., Meller, B. B., Morais, F. G., Mohr, C., Morgan, W., Nilsson, M. B., Peichl, M., Petäjä, T., Praß, M., Pöhlker, C., Pöhlker, M. L., Pöschl, U., Von Randow, C., Riipinen, I., Rinne, J., Rizzo, L. V., Rosenfeld, D., Silva Dias, M. A. F., Sogacheva, L., Stier, P., Swietlicki, E., Sörgel, M., Tunved, P., Virkkula, A., Wang, J., Weber, B., Yáñez-Serrano, A. M., Zieger, P., Mikhailov, E., Smith, J. N., and Kesselmeier, J.: Tropical and Boreal Forest – Atmosphere Interactions: A Review, Tellus B: Chemical and Physical Meteorology, 74, 24, https://doi.org/10.16993/tellusb.34, 2022.

Avissar, R., Silva Dias, P. L., Silva Dias, M. A. F., and Nobre, C.: The Large-Scale Biosphere-Atmosphere Experiment in Amazonia (LBA): Insights and future research needs, Journal of Geophysical Research: Atmospheres, 107, https://doi.org/10.1029/2002jd002704, 2002.

Biau, G. and Scornet, E.: A random forest guided tour, TEST, 25, 197–227, https://doi.org/10.1007/s11749-016-0481-7, 2016.

Blichner, S. M., Yli-Juuti, T., Mielonen, T., Pöhlker, C., Holopainen, E., Heikkinen, L., Mohr, C., Artaxo, P., Carbone, S., Meller, B. B., Quaresma Dias-Júnior, C., Kulmala, M., Petäjä, T., Scott, C. E., Svenhag, C., Nieradzik, L., Sporre, M., Partridge, D. G., Tovazzi, E., Virtanen, A., Kokkola, H., and Riipinen, I.: Process-evaluation of forest aerosol-cloud-climate feedback shows clear evidence from observations and large uncertainty in models, Nature Communications, 15, https://doi.org/10.1038/s41467-024-45001-y, 2024.

Bolton, D.: The Computation of Equivalent Potential Temperature, Monthly Weather Review, 108, 1046–1053, https://doi.org/10.1175/1520-0493(1980)108<1046:tcoept>2.0.co;2, 1980.

Botía, S., Komiya, S., Marshall, J., Koch, T., Gałkowski, M., Lavric, J., Gomes-Alves, E., Walter, D., Fisch, G., Pinho, D. M., Nelson, B. W., Martins, G., Luijkx, I. T., Koren, G., Florentie, L., Carioca de Araújo, A., Sá, M., Andreae, M. O., Heimann, M., Peters, W., and Gerbig, C.: The CO2 record at the Amazon Tall Tower Observatory: A new opportunity to study processes on seasonal and inter-annual scales, Global Change Biology, 28, 588–611, https://doi.org/10.1111/gcb.15905, 2021.

Braghiere, R. K., Yamasoe, M. A., Évora do Rosário, N. M., Ribeiro da Rocha, H., de Souza Nogueira, J., and de Araújo, A. C.: Characterization of the radiative impact of aerosols on CO2 and energy fluxes in the Amazon deforestation arch using artificial neural networks, Atmospheric Chemistry and Physics, 20, 3439–3458, https://doi.org/10.5194/acp-20-3439-2020, 2020.

Brito, J., Rizzo, L. V., Morgan, W. T., Coe, H., Johnson, B., Haywood, J., Longo, K., Freitas, S., Andreae, M. O., and Artaxo, P.: Ground-based aerosol characterization during the South American Biomass Burning Analysis (SAMBBA) field experiment, Atmospheric Chemistry and Physics, 14, 12 069–12 083, https://doi.org/10.5194/acp-14-12069-2014, 2014.

Cecchini, M. A., Albrecht, R. I., Andreae, M. O., Asperen, H. v., Artaxo, P., Bagheri, G., Balestra, G. G., Barbosa, C. G. G., Barbosa, H. M. J., Bighetto, A. S., Biscaro, T. S., Bodenschatz, E., Botía, S., Brito, L. P. d., Bueno, R. C., Calheiros, A. J. P., Camargo, L., Chiu, J. C., Conde, M., Costa, E. N. d., Dias-Júnior, C. Q., Faulhammer, P., Franco, M. A., Giangrande, S. E., Harder, H., Haytzmann, G. G., Herdies, D. L., Herdy, S., Jones, S. P., Kesselmeier, J., Lelieveld, J., Lopes, C. d. C., Lipken, F., Macêdo, T. L. B. d., Magina, F. C., Massafferri, A., Monteiro, C. d. A., Morais, F. G., Neofiti, M. C. S., Pöhlker, C., Pöhlker, M., Pöschl, U., Pugliesi, A. C., Raidiel, P. B., Quesada, C. A., Raj, S. S., Rizzo, L. V., Rossi, M. I., Sapucci, L. F., Saraiva, I., Seifert, P., Silva, F. A. G. d., Silva, D. F., Souza, R. A. F. d., Souza, C. M. A., Takeshi, B., Torres, A. B. S., Trumbore, S. E., Tsokankunku, A., Unfer, G. R., Valenti, W. I. D., Arellano, J. V.-G. d., Weber, B., Williams, C. R., Williams, J., and Machado, L. A. T.: The ATTO-Campina site: A new observatory for tropical convection and gas-aerosol-cloud-precipitation interactions in the Amazon, Bulletin of the American Meteorological Society, 106, BAMS–D–24–0092.1, https://doi.org/10.1175/BAMS-D-24-0092.1, 2025.

Cirino, G. G., Souza, R. A. F., Adams, D. K., and Artaxo, P.: The effect of atmospheric aerosol particles and clouds on net ecosystem exchange in the Amazon, Atmospheric Chemistry and Physics, 14, 6523–6543, https://doi.org/10.5194/acp-14-6523-2014, 2014.

Crous, K. Y., Middleby, K. B., Cheesman, A. W., Bouet, A. Y., Schiffer, M., Liddell, M. J., Barton, C. V., and Cernusak, L. A.: Leaf warming in the canopy of mature tropical trees reduced photosynthesis due to downregulation of photosynthetic capacity and reduced stomatal conductance, New Phytologist, 245, 1421–1436, https://doi.org/10.1111/nph.20320, 2025.

Davidson, E. A., de Araújo, A. C., Artaxo, P., Balch, J. K., Brown, I. F., C. Bustamante, M. M., Coe, M. T., DeFries, R. S., Keller, M., Longo, M., Munger, J. W., Schroeder, W., Soares-Filho, B. S., Souza, C. M., and Wofsy, S. C.: The Amazon basin in transition, Nature, 481, 321–328, https://doi.org/10.1038/nature10717, 2012.

de Menezes Neto, O. L., Coutinho, M. M., Marengo, J. A., and Capistrano, V. B.: The impacts of a plume-rise scheme on earth system modeling: climatological effects of biomass aerosols on the surface temperature and energy budget of South America, Theoretical and Applied Climatology, 129, 1035–1044, https://doi.org/10.1007/s00704-016-1821-y, 2016.

Dekker, S. C., Groenendijk, M., Booth, B. B. B., Huntingford, C., and Cox, P. M.: Spatial and temporal variations in plant water-use efficiency inferred from tree-ring, eddy covariance and atmospheric observations, Earth System Dynamics, 7, 525–533, https://doi.org/10.5194/esd-7-525-2016, 2016.

Deng, X., Zhang, J., Che, Y., Zhou, L., Lu, T., and Han, T.: The effect of diffuse radiation on ecosystem carbon fluxes across China from FLUXNET forest observations, Frontiers in Earth Science, 10, 906 408, https://doi.org/10.3389/feart.2022.906408, 2022.

Doughty, C. E., Flanner, M. G., and Goulden, M. L.: Effect of smoke on subcanopy shaded light, canopy temperature, and carbon dioxide uptake in an Amazon rainforest, Global Biogeochemical Cycles, 24, https://doi.org/10.1029/2009gb003670, 2010.

D'Oliveira, F. A., Cohen, J. C., Spracklen, D. V., Medeiros, A. S., Cirino, G. G., Artaxo, P., and Dias-Júnior, C. Q.: Simulation of the effects of biomass burning in a mesoscale convective system in the central amazon, Atmospheric Research, 278, 106 345, https://doi.org/10.1016/j.atmosres.2022.106345, 2022.

Eltbaakh, Y. A., Ruslan, M., Alghoul, M., Othman, M., Sopian, K., and Razykov, T.: Solar attenuation by aerosols: An overview, Renewable and Sustainable Energy Reviews, 16, 4264–4276, https://doi.org/10.1016/j.rser.2012.03.053, 2012.

Ezhova, E., Ylivinkka, I., Kuusk, J., Komsaare, K., Vana, M., Krasnova, A., Noe, S., Arshinov, M., Belan, B., Park, S.-B., et al.: Direct effect of aerosols on solar radiation and gross primary production in boreal and hemiboreal forests, Atmospheric Chemistry and Physics, 18, 17 863–17 881, https://doi.org/10.5194/acp-18-17863-2018, 2018.

Foken, T., Göockede, M., Mauder, M., Mahrt, L., Amiro, B., and Munger, W.: Post-Field Data Quality Control, pp. 181–208, Kluwer Academic Publishers, ISBN 1402022646, https://doi.org/10.1007/1-4020-2265-4_9, 2004.

Franco, M. A., Ditas, F., Kremper, L. A., Machado, L. A. T., Andreae, M. O., Araújo, A., Barbosa, H. M. J., de Brito, J. F., Carbone, S., Holanda, B. A., Morais, F. G., Nascimento, J. P., Pöhlker, M. L., Rizzo, L. V., Sá, M., Saturno, J., Walter, D., Wolff, S., Pöschl, U., Artaxo, P., and Pöhlker, C.: Occurrence and growth of sub-50 nm aerosol particles in the Amazonian boundary layer, Atmospheric Chemistry and Physics, 22, 3469–3492, https://doi.org/10.5194/acp-22-3469-2022, 2022.

Fratini, G. and Mauder, M.: Towards a consistent eddy-covariance processing: an intercomparison of EddyPro and TK3, Atmospheric Measurement Techniques, 7, 2273–2281, https://doi.org/10.5194/amt-7-2273-2014, 2014.

Fuzzi, S., Decesari, S., Facchini, M. C., Cavalli, F., Emblico, L., Mircea, M., Andreae, M. O., Trebs, I., Hoffer, A., Guyon, P., Artaxo, P., Rizzo, L. V., Lara, L. L., Pauliquevis, T., Maenhaut, W., Raes, N., Chi, X., Mayol-Bracero, O. L., Soto-García, L. L., Claeys, M., Kourtchev, I., Rissler, J., Swietlicki, E., Tagliavini, E., Schkolnik, G., Falkovich, A. H., Rudich, Y., Fisch, G., and Gatti, L. V.: Overview of the inorganic and organic composition of size-segregated aerosol in Rondônia, Brazil, from the biomass-burning period to the onset of the wet season, Journal of Geophysical Research: Atmospheres, 112, https://doi.org/10.1029/2005jd006741, 2007.

Gavrouzou, M., Hatzianastassiou, N., Korras-Carraca, M.-B., Stamatis, M., Lolis, C., Matsoukas, C., Michalopoulos, N., and Vardavas, I.: Three-Dimensional Distributions of the Direct Effect of anExtended and Intense Dust Aerosol Episode (16–18 June 2016) over the Mediterranean Basin on Regional Shortwave Radiation, Atmospheric Thermal Structure, and Dynamics, Applied Sciences, 13, 6878, https://doi.org/10.3390/app13126878, 2023.

Giles, D. M., Sinyuk, A., Sorokin, M. G., Schafer, J. S., Smirnov, A., Slutsker, I., Eck, T. F., Holben, B. N., Lewis, J. R., Campbell, J. R., Welton, E. J., Korkin, S. V., and Lyapustin, A. I.: Advancements in the Aerosol Robotic Network (AERONET) Version 3 database – automated near-real-time quality control algorithm with improved cloud screening for Sun photometer aerosol optical depth (AOD) measurements, Atmospheric Measurement Techniques, 12, 169–209, https://doi.org/10.5194/amt-12-169-2019, 2019.

Giorgi, F., Bi, X., and Qian, Y.: Direct radiative forcing and regional climatic effects of anthropogenic aerosols over East Asia: A regional coupled climate-chemistry/aerosol model study, Journal of Geophysical Research: Atmospheres, 107, AAC–7, https://doi.org/10.1029/2001JD001066, 2002.

Gomes Alves, E., Aquino Santana, R., Quaresma Dias-Júnior, C., Botía, S., Taylor, T., Yáñez-Serrano, A. M., Kesselmeier, J., Bourtsoukidis, E., Williams, J., Lembo Silveira de Assis, P. I., Martins, G., de Souza, R., Duvoisin Júnior, S., Guenther, A., Gu, D., Tsokankunku, A., Sörgel, M., Nelson, B., Pinto, D., Komiya, S., Martins Rosa, D., Weber, B., Barbosa, C., Robin, M., Feeley, K. J., Duque, A., Londoño Lemos, V., Contreras, M. P., Idarraga, A., López, N., Husby, C., Jestrow, B., and Cely Toro, I. M.: Intra- and interannual changes

in isoprene emission from central Amazonia, Atmospheric Chemistry and Physics, 23, 8149–8168, https://doi.org/10.5194/acp-23-8149-2023, 2023.

Gonçalves, W. A., Machado, L. A. T., and Kirstetter, P.-E.: Influence of biomass aerosol on precipitation over the Central Amazon: an observational study, Atmospheric Chemistry and Physics, 15, 6789–6800, https://doi.org/10.5194/acp-15-6789-2015, 2015.

Harriss, R. C., Wofsy, S. C., Garstang, M., Browell, E. V., Molion, L. C. B., McNeal, R. J., Hoell, J. M., Bendura, R. J., Beck, S. M., Navarro, R. L., Riley, J. T., and Snell, R. L.: The Amazon Boundary Layer Experiment (ABLE 2A): dry season 1985, Journal of Geophysical Research: Atmospheres, 93, 1351–1360, https://doi.org/10.1029/jd093id02p01351, 1988.

Herbert, R. and Stier, P.: Satellite observations of smoke–cloud–radiation interactions over the Amazon rainforest, Atmospheric Chemistry and Physics, 23, 4595–4616, https://doi.org/10.5194/acp-23-4595-2023, 2023.

Holanda, B. A., Franco, M. A., Walter, D., Artaxo, P., Carbone, S., Cheng, Y., Chowdhury, S., Ditas, F., Gysel-Beer, M., Klimach, T., Kremper, L. A., Krüger, O. O., Lavric, J. V., Lelieveld, J., Ma, C., Machado, L. A. T., Modini, R. L., Morais, F. G., Pozzer, A., Saturno, J., Su, H., Wendisch, M., Wolff, S., Pöhlker, M. L., Andreae, M. O., Pöschl, U., and Pöhlker, C.: African biomass burning affects aerosol cycling over the Amazon, Communications Earth amp; Environment, 4, https://doi.org/10.1038/s43247-023-00795-5, 2023.

Holton, J. R.: An introduction to dynamic meteorology, Academic Press, Amsterdam, 5. ed. edn., ISBN 9780123848666, includes bibliographical references and index, 2013.

Kanakidou, M., Myriokefalitakis, S., and Tsigaridis, K.: Aerosols in atmospheric chemistry and biogeochemical cycles of nutrients, Environmental Research Letters, 13, 063 004, https://doi.org/10.1088/1748-9326/aabcdb, 2018.

Kanniah, K. D., Beringer, J., North, P., and Hutley, L.: Control of atmospheric particles on diffuse radiation and terrestrial plant productivity: A review, Progress in Physical Geography: Earth and Environment, 36, 209–237, https://doi.org/10.1177/0309133311434244, 2012.

Karthick Raja Namasivayam, S., Priyanka, S., Lavanya, M., Krithika Shree, S., Francis, A., Avinash, G., Arvind Bharani, R., Kavisri, M., and Moovendhan, M.: A review on vulnerable atmospheric aerosol nanoparticles: Sources, impact on the health, ecosystem and management strategies, Journal of Environmental Management, 365, 121 644, https://doi.org/10.1016/j.jenvman.2024.121644, 2024.

Lau, K. M., Wu, H. T., Sud, Y. C., and Walker, G. K.: Effects of Cloud Microphysics on Tropical Atmospheric Hydrologic Processes and Intraseasonal Variability, Journal of Climate, 18, 4731–4751, https://doi.org/10.1175/jcli3561.1, 2005.

Li, H., Zhang, M., Wang, L., Su, X., and Lu, Y.: Effects of Different Types of Aerosols on Diffuse Radiation Based on Global AERONET, Journal of Geophysical Research: Atmospheres, 130, https://doi.org/10.1029/2024jd042701, 2025.

Liu, L., Cheng, Y., Wang, S., Wei, C., Pöhlker, M. L., Pöhlker, C., Artaxo, P., Shrivastava, M., Andreae, M. O., Pöschl, U., and Su, H.: Impact of biomass burning aerosols on radiation, clouds, and precipitation over the Amazon: relative importance of aerosol–cloud and aerosol–radiation interactions, Atmospheric Chemistry and Physics, 20, 13 283–13 301, https://doi.org/10.5194/acp-20-13283-2020, 2020.

Liu, Y., Flournoy, O., Zhang, Q., Novick, K. A., Koster, R. D., and Konings, A. G.: Canopy height and climate dryness parsimoniously explain spatial variation of unstressed stomatal conductance, Geophysical Research Letters, 49, e2022GL099 339, https://doi.org/10.1029/2022GL099339, 2022.

Lohmann, U. and Feichter, J.: Global indirect aerosol effects: a review, Atmospheric Chemistry and Physics, 5, 715–737, https://doi.org/10.5194/acp-5-715-2005, 2005.

Machado, L. A. T., Silva Dias, M. A. F., Morales, C., Fisch, G., Vila, D., Albrecht, R., Goodman, S. J., Calheiros, A. J. P., Biscaro, T., Kummerow, C., Cohen, J., Fitzjarrald, D., Nascimento, E. L., Sakamoto, M. S., Cunningham, C., Chaboureau, J.-P., Petersen, W. A., Adams, D. K., Baldini, L., Angelis, C. F., Sapucci, L. F., Salio, P., Barbosa, H. M. J., Landulfo, E., Souza, R. A. F., Blakeslee, R. J.,

Bailey, J., Freitas, S., Lima, W. F. A., and Tokay, A.: The Chuva Project: How Does Convection Vary across Brazil?, Bulletin of the American Meteorological Society, 95, 1365–1380, https://doi.org/10.1175/bams-d-13-00084.1, 2014.

Machado, L. A. T., Franco, M. A., Kremper, L. A., Ditas, F., Andreae, M. O., Artaxo, P., Cecchini, M. A., Holanda, B. A., Pöhlker, M. L., Saraiva, I., Wolff, S., Pöschl, U., and Pöhlker, C.: How weather events modify aerosol particle size distributions in the Amazon boundary layer, Atmospheric Chemistry and Physics, 21, 18 065–18 086, https://doi.org/10.5194/acp-21-18065-2021, 2021.

Malavelle, F. F., Haywood, J. M., Mercado, L. M., Folberth, G. A., Bellouin, N., Sitch, S., and Artaxo, P.: Studying the impact of biomass burning aerosol radiative and climate effects on the Amazon rainforest productivity with an Earth system model, Atmospheric Chemistry and Physics, 19, 1301–1326, https://doi.org/10.5194/acp-19-1301-2019, 2019.

Martin, S. T., Andreae, M. O., Althausen, D., Artaxo, P., Baars, H., Borrmann, S., Chen, Q., Farmer, D. K., Guenther, A., Gunthe, S. S., Jimenez, J. L., Karl, T., Longo, K., Manzi, A., Müller, T., Pauliquevis, T., Petters, M. D., Prenni, A. J., Pöschl, U., Rizzo, L. V., Schneider, J., Smith, J. N., Swietlicki, E., Tota, J., Wang, J., Wiedensohler, A., and Zorn, S. R.: An overview of the Amazonian Aerosol Characterization Experiment 2008 (AMAZE-08), Atmospheric Chemistry and Physics, 10, 11 415–11 438, https://doi.org/10.5194/acp-10-11415-2010, 2010.

Martin, S. T., Artaxo, P., Machado, L., Manzi, A. O., Souza, R. A. F., Schumacher, C., Wang, J., Biscaro, T., Brito, J., Calheiros, A., Jardine, K., Medeiros, A., Portela, B., de Sá, S. S., Adachi, K., Aiken, A. C., Albrecht, R., Alexander, L., Andreae, M. O., Barbosa, H. M. J., Buseck, P., Chand, D., Comstock, J. M., Day, D. A., Dubey, M., Fan, J., Fast, J., Fisch, G., Fortner, E., Giangrande, S., Gilles, M., Goldstein, A. H., Guenther, A., Hubbe, J., Jensen, M., Jimenez, J. L., Keutsch, F. N., Kim, S., Kuang, C., Laskin, A., McKinney, K., Mei, F., Miller, M., Nascimento, R., Pauliquevis, T., Pekour, M., Peres, J., Petäjä, T., Pöhlker, C., Pöschl, U., Rizzo, L., Schmid, B., Shilling, J. E., Dias, M. A. S., Smith, J. N., Tomlinson, J. M., Tóta, J., and Wendisch, M.: The Green Ocean Amazon Experiment (GoAmazon2014/5) Observes Pollution Affecting Gases, Aerosols, Clouds, and Rainfall over the Rain Forest, Bulletin of the American Meteorological Society, 98, 981–997, https://doi.org/10.1175/bams-d-15-00221.1, 2017.

Mauder, M., Jung, M., Stoy, P., Nelson, J., and Wanner, L.: Energy balance closure at FLUXNET sites revisited, Agricultural and Forest Meteorology, 358, 110 235, https://doi.org/10.1016/j.agrformet.2024.110235, 2024.

Mercado, L. M., Bellouin, N., Sitch, S., Boucher, O., Huntingford, C., Wild, M., and Cox, P. M.: Impact of changes in diffuse radiation on the global land carbon sink, Nature, 458, 1014–1017, https://doi.org/10.1038/nature07949, 2009.

Meyers, T. P. and Dale, R. F.: Predicting Daily Insolation with Hourly Cloud Height and Coverage, Journal of Climate and Applied Meteorology, 22, 537–545, https://doi.org/10.1175/1520-0450(1983)022<0537:pdiwhc>2.0.co;2, 1983.

Miller, R. L., Tegen, I., and Perlwitz, J.: Surface radiative forcing by soil dust aerosols and the hydrologic cycle, Journal of Geophysical Research: Atmospheres, 109, https://doi.org/10.1029/2003jd004085, 2004.

Morais, F. G., Franco, M. A., Palácios, R., Machado, L. A. T., Rizzo, L. V., Barbosa, H. M. J., Jorge, F., Schafer, J. S., Holben, B. N., Landulfo, E., and Artaxo, P.: Relationship between Land Use and Spatial Variability of Atmospheric Brown Carbon and Black Carbon Aerosols in Amazonia, Atmosphere, 13, https://doi.org/10.3390/atmos13081328, 2022.

Moreira, D. S., Longo, K. M., Freitas, S. R., Yamasoe, M. A., Mercado, L. M., Rosário, N. E., Gloor, E., Viana, R. S. M., Miller, J. B., Gatti, L. V., Wiedemann, K. T., Domingues, L. K. G., and Correia, C. C. S.: Modeling the radiative effects of biomass burning aerosols on carbon fluxes in the Amazon region, Atmospheric Chemistry and Physics, 17, 14 785–14 810, https://doi.org/10.5194/acp-17-14785-2017, 2017.

NASA JPL: NASADEM Merged DEM Global 1 arc second V001, [Data set], https://doi.org/10.5067/MEaSUREs/NASADEM/NASADEM_HGT.001, accessed 2020-12-30, 2020.

Orsini, C. Q., Tabacniks, M. H., Artaxo, P., Andrade, M. F., and Kerr, A. S.: Characteristics of fine and coarse particles of natural and urban aerosols of Brazil, Atmospheric Environment, 20, 2259–2269, https://doi.org/10.1016/0004-6981(86)90316-1, 1896.

Palácios, R., Castagna, D., Barbosa, L., Souza, A. P., Imbiriba, B., Zolin, C. A., Nassarden, D., Duarte, L., Morais, F. G., Franco, M. A., Cirino, G., Kuhn, P., Sodré, G., Curado, L., Basso, J., Roberto de Paulo, S., and Rodrigues, T.: ENSO effects on the relationship between aerosols and evapotranspiration in the south of the Amazon biome, Environmental Research, 250, 118 516, https://doi.org/10.1016/j.envres.2024.118516, 2024.

Palácios, R. d. S., Morais, F. G., Landulfo, E., Franco, M. A. d. M., Kuhnen, I. A., Marques, J. B., Nogueira, J. d. S., Júnior, L. C. G. d. V., Rodrigues, T. R., Romera, K. S., Curado, L. F. A., Banga, N. M., Rothmund, L. D., Sallo, F. d. S., Morais, D., Santos, A. C. A., and Moraes, T. J.: Long Term Analysis of Optical and Radiative Properties of Aerosols in the Amazon Basin, Aerosol and Air Quality Research, 20, 139–154, https://doi.org/10.4209/aaqr.2019.04.0189, 2020.

Palácios, R. d. S., Artaxo, P., Cirino, G. G., Nakale, V., Morais, F. G., Rothmund, L. D., Biudes, M. S., Machado, N. G., Curado, L. F. A., Marques, J. B., and Nogueira, J. d. S.: Long-term measurements of aerosol optical properties and radiative forcing (2011-2017) over Central Amazonia, Atmósfera, 35, 143–163, https://doi.org/10.20937/atm.52892, 2022.

Pareja-Quispe, D., Franchito, S. H., and Fernandez, J. P. R.: Assessment of the RegCM4 Performance in Simulating the Surface Radiation Budget and Hydrologic Balance Variables in South America, Earth Systems and Environment, 5, 499–518, https://doi.org/10.1007/s41748-021-00249-y, 2021.

Pillai, K. C. S.: Some New Test Criteria in Multivariate Analysis, The Annals of Mathematical Statistics, 26, 117–121, https://doi.org/10.1214/aoms/1177728599, 1955.

Procopio, A. S., Artaxo, P., Kaufman, Y. J., Remer, L. A., Schafer, J. S., and Holben, B. N.: Multiyear analysis of amazonian biomass burning smoke radiative forcing of climate, Geophysical Research Letters, 31, https://doi.org/10.1029/2003gl018646, 2004.

Pöhlker, C., Walter, D., Paulsen, H., Könemann, T., Rodríguez-Caballero, E., Moran-Zuloaga, D., Brito, J., Carbone, S., Degrendele, C., Després, V. R., Ditas, F., Holanda, B. A., Kaiser, J. W., Lammel, G., Lavrič, J. V., Ming, J., Pickersgill, D., Pöhlker, M. L., Praß, M., Löbs, N., Saturno, J., Sörgel, M., Wang, Q., Weber, B., Wolff, S., Artaxo, P., Pöschl, U., and Andreae, M. O.: Land cover and its transformation in the backward trajectory footprint region of the Amazon Tall Tower Observatory, Atmospheric Chemistry and Physics, 19, 8425–8470, https://doi.org/10.5194/acp-19-8425-2019, 2019.

Pöhlker, M. L., Pöhlker, C., Ditas, F., Klimach, T., Hrabe de Angelis, I., Araújo, A., Brito, J., Carbone, S., Cheng, Y., Chi, X., Ditz, R., Gunthe, S. S., Kesselmeier, J., Könemann, T., Lavrič, J. V., Martin, S. T., Mikhailov, E., Moran-Zuloaga, D., Rose, D., Saturno, J., Su, H., Thalman, R., Walter, D., Wang, J., Wolff, S., Barbosa, H. M. J., Artaxo, P., Andreae, M. O., and Pöschl, U.: Long-term observations of cloud condensation nuclei in the Amazon rain forest – Part 1: Aerosol size distribution, hygroscopicity, and new model parametrizations for CCN prediction, Atmospheric Chemistry and Physics, 16, 15 709–15 740, https://doi.org/10.5194/acp-16-15709-2016, 2016.

Pöhlker, M. L., Ditas, F., Saturno, J., Klimach, T., Hrabě de Angelis, I., Araùjo, A. C., Brito, J., Carbone, S., Cheng, Y., Chi, X., Ditz, R., Gunthe, S. S., Holanda, B. A., Kandler, K., Kesselmeier, J., Könemann, T., Krüger, O. O., Lavrič, J. V., Martin, S. T., Mikhailov, E., Moran-Zuloaga, D., Rizzo, L. V., Rose, D., Su, H., Thalman, R., Walter, D., Wang, J., Wolff, S., Barbosa, H. M. J., Artaxo, P., Andreae, M. O., Pöschl, U., and Pöhlker, C.: Long-term observations of cloud condensation nuclei over the Amazon rain forest – Part 2: Variability and characteristics of biomass burning, long-range transport, and pristine rain forest aerosols, Atmospheric Chemistry and Physics, 18, 10 289–10 331, https://doi.org/10.5194/acp-18-10289-2018, 2018.

RAISG: Geospatial Vetor Data of the biomes, limits and cities, [Data set], https://www.raisg.org/en/maps/, accessed: 2023-12-01, 2023.

Ramanathan, V., Crutzen, P. J., Kiehl, J. T., and Rosenfeld, D.: Aerosols, Climate, and the Hydrological Cycle, Science, 294, 2119–2124, https://doi.org/10.1126/science.1064034, 2001.

Rap, A., Scott, C. E., Spracklen, D. V., Bellouin, N., Forster, P. M., Carslaw, K. S., Schmidt, A., and Mann, G.: Natural aerosol direct and indirect radiative effects, Geophysical Research Letters, 40, 3297–3301, https://doi.org/10.1002/grl.50441, 2013.

Rap, A., Spracklen, D. V., Mercado, L., Reddington, C. L., Haywood, J. M., Ellis, R. J., Phillips, O. L., Artaxo, P., Bonal, D., Restrepo Coupe, N., and Butt, N.: Fires increase Amazon forest productivity through increases in diffuse radiation, Geophysical Research Letters, 42, 4654–4662, https://doi.org/10.1002/2015gl063719, 2015.

Rizzo, L. V., Correia, A. L., Artaxo, P., Procópio, A. S., and Andreae, M. O.: Spectral dependence of aerosol light absorption over the Amazon Basin, Atmospheric Chemistry and Physics, 11, 8899–8912, https://doi.org/10.5194/acp-11-8899-2011, 2011.

Rodrigues, S., Cirino, G., Moreira, D., Pozzer, A., Palácios, R., Lee, S.-C., Imbiriba, B., Nogueira, J., Vitorino, M. I., and Vourlitis, G.: Enhanced net CO2 exchange of a semideciduous forest in the southern Amazon due to diffuse radiation from biomass burning, Biogeosciences, 21, 843–868, https://doi.org/10.5194/bg-21-843-2024, 2024.

Ross, J. L., Hobbs, P. V., and Holben, B.: Radiative characteristics of regional hazes dominated by smoke from biomass burning in Brazil: Closure tests and direct radiative forcing, Journal of Geophysical Research: Atmospheres, 103, 31 925–31 941, https://doi.org/10.1029/97jd03677, 1998.

Santana, R. A. S. d., Vale, R. S. d., Silva, J. T. d., Santos, R. M. N. d., Fitzjarrald, D. R., Picanço, G. A. d. S., Batalha, S. S. A., Gomes, A. C. d. S., Costa, G. B., Tapajós, R., and Silva, R. D.: Wind averages features above and below of the forest canopy during GoAmazon in an experimental site in the Amazon, Ciência e Natura, 38, 152, https://doi.org/10.5902/2179460x20131, 2016.

Schmitt, A. U., Ament, F., de Araújo, A. C., Sá, M., and Teixeira, P.: Modeling atmosphere–land interactions at a rainforest site – a case study using Amazon Tall Tower Observatory (ATTO) measurements and reanalysis data, Atmospheric Chemistry and Physics, 23, 9323–9346, https://doi.org/10.5194/acp-23-9323-2023, 2023.

Seinfeld, J. H. and Pandis, S. N.: Atmospheric Chemistry and Physics, Wiley-Interscience, [s.l.], 2. aufl. edn., ISBN 0471720186, description based upon print version of record, 2006.

Seinfeld, J. H. and Pandis, S. N.: Atmospheric chemistry and physics: from air pollution to climate change, John Wiley & Sons, 2016.

Sena, E. T., Artaxo, P., and Correia, A. L.: Spatial variability of the direct radiative forcing of biomass burning aerosols and the effects of land use change in Amazonia, Atmospheric Chemistry and Physics, 13, 1261–1275, https://doi.org/10.5194/acp-13-1261-2013, 2013.

Steiner, A. L., Mermelstein, D., Cheng, S. J., Twine, T. E., and Oliphant, A.: Observed Impact of Atmospheric Aerosols on the Surface Energy Budget, Earth Interactions, 17, 1–22, https://doi.org/10.1175/2013ei000523.1, 2013.

Suzuki, K., Stephens, G. L., and Golaz, J.: Significance of aerosol radiative effect in energy balance control on global precipitation change, Atmospheric Science Letters, 18, 389–395, https://doi.org/10.1002/asl.780, 2017.

Tetens, O.: Uber einige meteorologische Begriffe, Z. Geophys, 6, 297–309, https://cir.nii.ac.jp/crid/1571698600341727488, 1930.

von Randow, C., Manzi, A. O., Kruijt, B., de Oliveira, P. J., Zanchi, F. B., Silva, R. L., Hodnett, M. G., Gash, J. H. C., Elbers, J. A., Waterloo, M. J., Cardoso, F. L., and Kabat, P.: Comparative measurements and seasonal variations in energy and carbon exchange over forest and pasture in South West Amazonia, Theoretical and Applied Climatology, 78, https://doi.org/10.1007/s00704-004-0041-z, 2004.

Wang, S. and Yi, B.: Bibliometric Analysis of Aerosol-Radiation Research from 1999 to 2023, Atmosphere, 15, 1189, https://doi.org/10.3390/atmos15101189, 2024.

Wilks, D. S.: Statistical methods in the atmospheric sciences, vol. 100, Academic press, 2011.

Yamasoe, M. A., von Randow, C., Manzi, A. O., Schafer, J. S., Eck, T. F., and Holben, B. N.: Effect of smoke and clouds on the transmissivity of photosynthetically active radiation inside the canopy, Atmospheric Chemistry and Physics, 6, 1645–1656, https://doi.org/10.5194/acp-6-1645-2006, 2006.

Yang, Y., Guan, H., Batelaan, O., McVicar, T. R., Long, D., Piao, S., Liang, W., Liu, B., Jin, Z., and Simmons, C. T.: Contrasting responses of water use efficiency to drought across global terrestrial ecosystems, Scientific Reports, 6, https://doi.org/10.1038/srep23284, 2016.

Yokelson, R. J., Karl, T., Artaxo, P., Blake, D. R., Christian, T. J., Griffith, D. W. T., Guenther, A., and Hao, W. M.: The Tropical Forest and Fire Emissions Experiment: overview and airborne fire emission factor measurements, Atmospheric Chemistry and Physics, 7, 5175–5196, https://doi.org/10.5194/acp-7-5175-2007, 2007.

Zhang, Y., Fu, R., Yu, H., Dickinson, R. E., Juarez, R. N., Chin, M., and Wang, H.: A regional climate model study of how biomass burning aerosol impacts land-atmosphere interactions over the Amazon, Journal of Geophysical Research: Atmospheres, 113, https://doi.org/10.1029/2007jd009449, 2008.